Charles University

Faculty of Science

Department of Physical and Macromolecular Chemistry

Study programme: Macromolecular Chemistry

Bc. Filip Steiner

Boron Cluster Conjugates as Building Blocks for the Preparation of Polymeric Nanostructures

Konjugáty klastrů bóru jako stavební bloky pro přípravu polymerních nanostruktur

Diploma thesis

Supervisor: prof. RNDr. Pavel Matějíček, Ph.D.

Advisor: Ing. Mariusz Uchman, Ph.D.

Prague, 2023

Declaration

With this, I declare that I have carried out the work independently. I proclaim that I have cited all references and literature properly. Neither this work nor a substantial part was submitted elsewhere to obtain an academic degree.

Prague, 9th August 2023

Prohlášení

Prohlašuji, že jsem závěrečnou práci zpracoval samostatně a že jsem uvedl všechny použité informační zdroje a literaturu. Tato práce ani její podstatná část nebyla předložena k získání jiného nebo stejného akademického titulu.

V Praze, 09.08.2023

Bc. Filip Steiner, v. r.

Acknowledgements

First and foremost, I would like to thank my supervisor Prof. Pavel Matějíček for his guidance, valuable advice, and cooperation during my past five years in the Soft Matter group at the Department of Physical and Macromolecular Chemistry. Also, I would like to show my gratitude to all current and former members of the group with whom I could work and who showed me not only the beauty of the chemistry of the exotic boron cluster compounds but also that I could work in such a friendly work environment (I will miss especially Wednesdays cleaning sessions).

I want to thank Dr. Zdeněk Tošner from the NMR lab for measuring ^{1}H DOSY NMR spectra. Also, I would like to thank Dr. Petr Cígler from IOCB Prague for the suggestions on the purification of boron cluster dumbbells and for the ion exchange resin.

Last but not least, I would like to thank my family and friends for their love and support, especially to my emergency contacts, whom I could reach whenever I needed. I would not be able to do what I like without you.

To whom it may concern, thank you very much.

The author gratefully acknowledges the financial support of the Czech Science Foundation (GAČR) grant No. 21-20008K.

Charles University in Prague

Faculty of Science

Department of Physical and Macromolecular Chemistry

Author: Bc. Filip Steiner

Supervisor: prof. RNDr. Pavel Matějíček, Ph.D.

Advisor: Ing. Mariusz Uchman, Ph.D.

Title: Boron Cluster Conjugates as Building Blocks for the Preparation of Polymeric Nanostructures

Abstract

This diploma thesis investigates the synthesis and supramolecular behaviour of amphiphilic conjugates of closo-dodecaborate dianion, $[B_{12}H_{12}]^{2-}$, with polycationic diblock copolymer poly(ethylene oxide)-*block*-poly(2-(*N*, *N*, *N*', *N*'-tetramethyl guanidium ethyl acrylate), PEO_n-*b*-$PGEA_m$. The boron cluster dumbbells were synthesised by the exoskeletal, electrophile-induced nucleophilic substitution (EINS) and by subsequently ring-opening reaction with various aliphatic diols, resulting in a hybrid dumbbell molecule. These molecules were used for preparation of nanoparticles by co-assembly with polycationic diblock copolymer in water. Resulted nanostructures were characterised by static and dynamic light scattering and NMR spectroscopy.

Keywords: boron cluster compounds, polymeric nanoparticles, co-assembly, NMR, light scattering

Univerzita Karlova v Praze

Přírodovědecká fakulta

Katedra fyzikální a makromolekulární chemie

Autor: Bc. Filip Steiner

Vedoucí práce: prof. RNDr. Pavel Matějíček, Ph.D.

Konzultant: Ing. Mariusz Uchman, Ph.D.

Název diplomové práce: Konjugáty klastrů bóru jako stavební bloky pro přípravu polymerních nanostruktur

Abstrakt

Tato diplomová práce se zabývá syntézou a supramolekulárním chováním amfifilních konjugátů *closo*-dodekaborátového dianiontu, $[B_{12}H_{12}]^{2-}$, s polykationtovým diblokovým kopolymerem poly(ethylen oxid)-*b*-poly(2-(*N*, *N*, *N*', *N*'-tetramethylguanidium ethylakrylát), PEO_n-*b*-$PGEA_m$. Konjugáty klastrů bóru byly syntetizovány pomocí exoskeletální, elektrofilem indukované nukleofilní substituce (EINS) a následnou reakcí s různými alifatickými dioly, což vedlo ke vzniku amfifilních molekul činkovitého tvaru. Ty byly následně využity k přípravě nanočástic spoluskládáním s polykationtovými blokovými kopolymery ve vodě. Výsledné nanostruktury byly charakterizovány pomocí statického a dynamického rozptylu světla a spektroskopie NMR.

Klíčová slova: klastrové sloučeniny bóru, polymerní nanočástice, spoluskládání, NMR, rozptyl světla

Table of Contents

Abbreviations

2*c*-2*e*	Two-centre two-electron
3*c*-2*e*	Three-centre two-electron
AANS	Acid-assisted nucleophilic substitution
AIDS	Acquired immune deficiency syndrome
AOs	Atomic orbitals
BCCs	Boron cluster compounds
BNCT	Boron neutron capture therapy
BPA	L-*p*-dihydroxyborylphenylalanine
BSH	Sodium mercaptododecaborate
CMC	Critical micelle concentration
CONTIN	Constrained inverse Laplace transform routine
COSAN	Cobalt sandwich; cobalt(III) bis(1,2-dicarbollide) anion (1-)
DOSY	Diffusion ordered spectroscopy
DLS	Dynamic light scattering
EINS	Electrophile-induced nucleophile substitution
ESI-MS	Electrospray ionisation mass spectrometry
FESAN	Iron sandwich; iron(III) bis(1,2-dicarbollide) anion (1-)
HIV	Human Immunodeficiency virus
Hz	Hertz
LCAO	Linear combination of atomic orbitals
LS	Light scattering
MOs	Molecular orbitals

NICS	Nucleus-independent chemical shift
NISAN	Nickel sandwich; nickel(III, IV) bis(1,2-dicarbollide) anion (1-)
NMR	Nuclear magnetic resonance
PEO_n-*b*-$PGEA_m$	poly(ethylene oxide)-*block*-poly(2-(*N*, *N*, *N*', *N*'-tetramethyl guanidium ethyl acrylate)
ppm	Parts per million
RAFT	Reversible addition-fragmentation chain-transfer
RNA	Ribonucleic acid
SLS	Static light scattering
XRD	X-ray diffraction

1 Introduction and Aims of the Thesis

Boron cluster compounds and their derivatives are inorganic compounds containing multiple boron and hydrogen atoms bonded together in a cluster formation. These compounds have attracted significant attention due to their unique chemical and physical properties.

The history of borane compounds began in the early 1910s with the pioneering work of German chemist Alfred Stock and the synthesis of diborane. But it was not until the 1950s and 1960s, with the discovery of anionic polyhedral boron clusters and their derivatives, that the field of boron chemistry truly began to expand and evolve. This was primarily because of their exceptionally high thermal and chemical stability compared with those of electron-neutral boranes, synthesised at the beginning of the twentieth century. Today, boranes and their derivatives continue to be an active area of research with potential applications in various fields such as medicine (BNCT, imaging, drug delivery, or antiviral and antimicrobial activity), materials (ionic liquids, liquid crystals, nonlinear optics, or ion batteries) catalysis, environment (extraction of radionuclides from radioactive waste) or in the preparation of nanostructures.

This diploma thesis is aimed at one of the most stable polyhedral anionic boron clusters – *closo*-dodecaborate anion (2-), $[B_{12}H_{12}]^{2-}$, and its use as a building block for the preparation of nanostructures. The aims of the thesis could be summarised in the following points:

- Synthesis of boron cluster conjugates via ring-opening reaction of the cyclic oxonium conjugate of *closo*-dodecaborate anion (2-) and 1,4-dioxane with different diols.

- Study the formation of nanoparticles or other nanostructures based on the co-assembly of prepared conjugates of boron cluster compounds with polycationic diblock copolymers in water using physicochemical techniques, such as NMR spectroscopy and static and dynamic light scattering.

2 Overview of the Literature

2.1 Boron cluster compounds

Boron cluster compounds are three-dimensional inorganic clusters composed of boron atoms. This group of compounds is relatively abundant since boron, like, e.g., carbon, sulphur, or silicon, can be chained by connecting the atoms of the given element.[1] The most studied species are boron hydrides (boranes), carboranes, metallacarboranes and their derivatives.

2.1.1 Boranes

Boranes are inorganic compounds consisting only of boron and hydrogen atoms. Boranes are considered electron-deficient clusters, i.e., species with fewer valence electrons than are required for a localised bonding scheme, and atoms form cage-like structures.[2] The simplest borane is borohydride anion, $[BH_4]^-$, which is isoelectronic with methane molecule and ammonium cation. From 1912 to 1936, Alfred Stock's pioneering work showed that boron could form a variety of hydrides with different properties.[3, 4] The examples of boron hydrides molecules are shown in Figure 2.1:

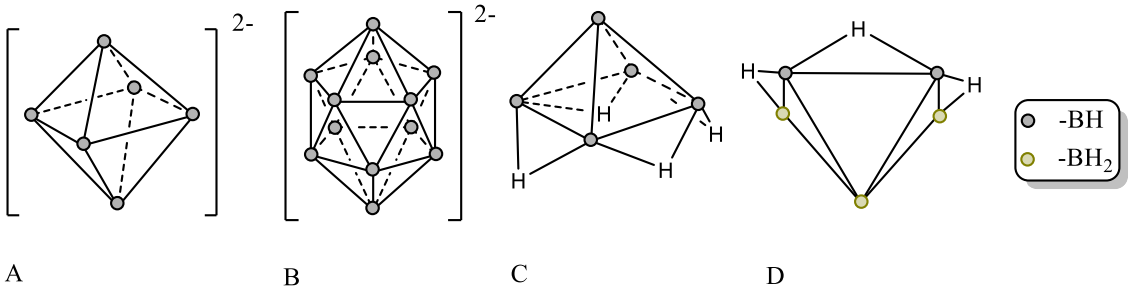

Figure 2.1 The examples of boron hydrides; A: *closo*-$[B_6H_6]^{2-}$, B: *closo*-$[B_{12}H_{12}]^{2-}$, C: *nido*-B_5H_9, D: *arachno*-B_5H_{11}.

2.1.1.1 Chemical properties

Boranes are colourless, diamagnetic molecular compounds. Lower boron hydrides are gases at room temperature, but they become volatile liquids and solids with increasing molecular weight.[5] The first synthesised boranes were electron-neutral species containing fewer boron atoms incorporated in a cluster formation. These molecules are very reactive; some could spontaneously combust in the air. High reactivity of electron-neutral boranes is caused by the presence of B-H-B and BH_2 groups, which are hydrogen-rich. Higher electron-neutral boron hydrides and anionic boranes, first synthesised by M. F. Hawthorne and A. R. Pitochelli in the 1960s [4], are, on the other hand, very stable and

primarily unreactive toward oxygen, water, or high temperatures. The stabilisation of those clusters could explain this increased stability via three-dimensional aromaticity, which occurs in the molecules.[6]

2.1.1.2 Bonding and Structure

The structure of boron hydrides was explored in the 1940s. The XRD measurements of *nido*-decaborane revealed that this molecule contains four bridging hydrogen atoms and a deltahedral skeleton formed by ten boron atoms. Subsequently, the bridging hydrogen atoms were also found in the structures of diborane and *nido*-pentaborane. These findings proved the presence of two different types of bonding in boron hydrides: the common two-centre two-electron (2*c*-2*e*) bonds and the three-centre two-electron (3*c*-2*e*) bonds. The idea of three-centre bonding was extensively developed by W. N. Lipscomb, Nobel Prize laureate in 1976, *for his studies on the structure of boranes illuminating problems of chemical bonding*.[7]

In the case of 2*c*-2*e* bonds, molecular orbitals (MOs) are formed by a linear combination of atomic orbitals (LCAO), creating one bonding orbital and one antibonding orbital. On the other hand, the 3*c*-2*e* bond is formed by the interaction of 3 AOs which include one bonding and two antibonding orbitals. A few criteria determine whether AOs could be combined to form MOs in the 3*c*-2*e* bonds: they must be similar in energy, there has to be a spatial overlap and appropriate symmetry is required. In the boron hydride molecules, two types of 3*c*-2*e* bonds occur: bridge B-H-B bonds and central B-B-B bonds.[5, 7, 8] 3*c*-2*e* bonds occur in molecules with fewer bonding electrons than atomic orbital. Because of that, these structures are also called electron-deficient structures.[9]

The shape of boron hydrides could be determined by PSEPT (*polyhedral skeletal electron pair theory*), developed by Wade, Williams and Mingos. From this theory, empirical rules, also called Wade's or Wade – Mingo's rules, follow. According to structure, boron hydrides and their derivatives can be divided as follows: [1, 2, 10, 11]

- *Closo*-clusters (a corruption of *clovo*, from Latin clovis, meaning *cage*), $[B_nH_n]^{2-}$ (n = 6 – 12). These compounds form a deltahedral cage of n boron atoms (a deltahedron is a polyhedron that possesses only triangular faces, e. g. an octahedron or an icosahedron). *Closo*-cluster with n vertices must contain (n + 1) electron pairs which occupy (n + 1) bonding MOs.

- *Nido*-clusters (from Latin *nidus*, meaning *nest*), B_nH_{n+4}, $[B_nH_{n+3}]^-$. The cluster's shape is derived from the original *closo*-cluster with *n* vertices and has (n – 1) vertices and (n + 1) pairs of electrons.
- *Arachno*-clusters (from Greek, meaning *spider's web*), B_nH_{n+6}, $[B_nH_{n+5}]^-$. These clusters are very reactive, derived from the original *closo*-cluster and have (n – 2) vertex and (n + 1) pairs of electrons.
- *Hypho*-clusters (from Greek, meaning *to weave* or *a net*), B_nH_{n+8}, $[B_nH_{n+7}]^-$. This is a poorly exemplified group of borane clusters, and it is derived from the original *closo*-cluster with (n – 3) vertex and (n + 1) pairs of electrons.
- *Klado*-clusters (from Greek, meaning *branch*), B_nH_{n+10}, $[B_nH_{n+9}]^-$. Also, like *hypho*-clusters, this group of boron hydrides is only very poorly exemplified. *Klado*-clusters are derived from the original *closo*-cluster and have (n – 4) vertex and (n + 1) pairs of electrons.

A *conjuncto*-clusters (Latin, meaning *join together*) are not derived from Wade's rules, but this is a typical cluster type formed by two or more cluster skeletons connected by a joint atom, edge, or surface. Derivation of clusters based on the Wade's rules is shown in Figure 2.2.

Figure 2.2 Derivation of *nido*-, *arachno*-, *hypho*- and *klado*-clusters from the original icosahedral *closo*-cluster according to Wade's rules.

2.1.1.3 Three-dimensional aromaticity

One of the reasons for the exceptionally high stability of anionic boron hydrides is the phenomenon of three-dimensional aromaticity, which occurs in these molecules. Sigma bond interactions drive the aromatic behaviour in boranes compared to aromatic hydrocarbons, where π-bonds play an essential role. Aromaticity in polyhedral boron hydrides was studied theoretically [12, 13] and proven experimentally by multiple methods.

In NMR studies, measurements of nucleus-independent chemical shift (NICS), which is nowadays the most used method for studying aromaticity, were used. Secondly, the measurements of the magnetic susceptibility (χ) were taken. Values obtained from these experiments have shown the aromatic behaviour of polyhedral boron hydrides.[14] Also, the high stability of these compounds supported the idea of aromaticity in boranes. Another proof of aromaticity in polyhedral boranes is that boron cluster compounds undergo chemical reactions typical for aromatic compounds. Besides the *closo*-cluster, open clusters, such as *nido*- and *arachno*-clusters, also show aromatic behaviour. However, a lower aromatic behaviour is observed because of less electron delocalisation caused by an open cluster cage.[6, 15, 16]

2.1.2 Carboranes and metallacarboranes

Carboranes (formally carbaboranes) are the most studied class of hetero-boranes (boranes, where one or more [BH] fragments in the cluster vertex are substituted with hetero atom, e.g., carbon, sulphur, phosphorus, or oxygen, with conservation of an original number of vertex or valence electrons). These compounds have been known since the mid-1950s. Theoretically, they had been predicted by Lipscomb and Hoffmann.[17,18,19] Similarly to the boron hydrides, the structure of the carboranes could be derived from Wade's rules.[10] Although the first carboranes were synthesised in the 1950s, they were not reported in the literature since the 1960s. The reason for that was U.S. post-World War II research aiming at developing borane-based aircraft fuels.[6] The most studied carborane species are icosahedral, 12 vertex boranes derivates containing one or two [CH] fragments incorporated into the cluster framework. This is primarily because of their high stability. The dicarboranes (carboranes containing 2 [CH] fragments) exist in 3 different isomers. Firstly, they were synthesised in 1957 by the reaction of *nido*-$B_{10}H_{14}$ with acetylene.[20, 21] The examples of varying carborane species are shown in Figure 2.3.

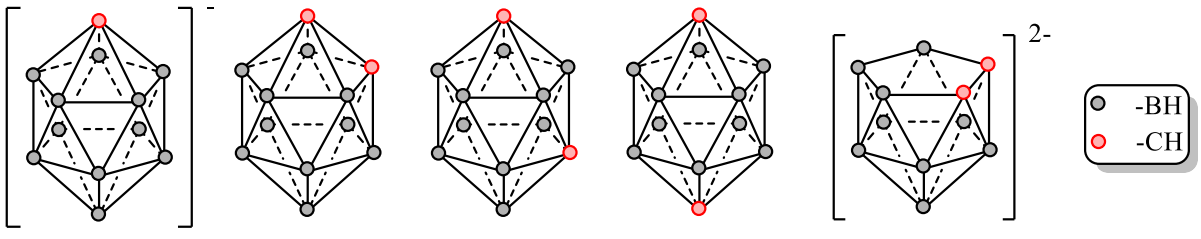

$[CB_{11}H_{12}]^-$ | 1,2-$C_2B_{10}H_{12}$ (*ortho*) | 1,7-$C_2B_{10}H_{12}$ (*meta*) | 1,12-$C_2B_{10}H_{12}$ (*para*) | *nido*-$[7,8\text{-}C_2B_9H_{11}]^{2-}$ (dicarbollide)

Figure 2.3 Examples of carborane molecules.

In 1964 Hawthorne and co-workers showed that *closo*-dicarboranes react with strong bases in a suitable solvent (such as ethanol), forming the *nido*-dicarborane anion (1-). This reaction was observed only with ortho and para isomers of $C_2B_{10}H_{12}$.[5, 22] Afterwards, *nido*-dicarborane anion (1-) reacts by splitting off the bridging hydrogen atom, resulting in *nido*-dicarbollide anion (2-) (structure in Figure 2.3), which behaves as η^5-ligand, similar to cyclopentadienyl anion. This ligand reacts with various transition metals (such as Co, Fe, Ni, or Pd)[23, 24, 25, 26] and forms so-called sandwich complexes known as metallacarboranes. The most known sandwich complex is cobalt(III) bis(1,2-dicarbollide) anion (1-), also called COSAN (derived from CObalt SANdwich). Other well-known metallacarboranes are iron(III) bis(1,2-dicarbollide) anion (1-) (FESAN) or nickel(III, IV) bis(1,2-dicarbollide) anion (1-) (NISAN). In structure are metallacarboranes like the metallocenes, whereas ligand is featured cyclopentadienyl anion. The main difference between those two types of complexes is the strength of the ligand-metal bond, which is more covalent in metallacarboranes. This leads to a stronger bonding and higher stability of metallacarboranes compared to metallocenes.[6, 27, 28] Metallacarboranes exist in numerous rotamers, which differ in energy levels.[29] The conformation of metallacarboranes can be affected by various external stimuli, such as the type of counterion or functional groups attached to the cluster.[30] The structures of metallacarboranes rotamers are shown in Figure 2.4.

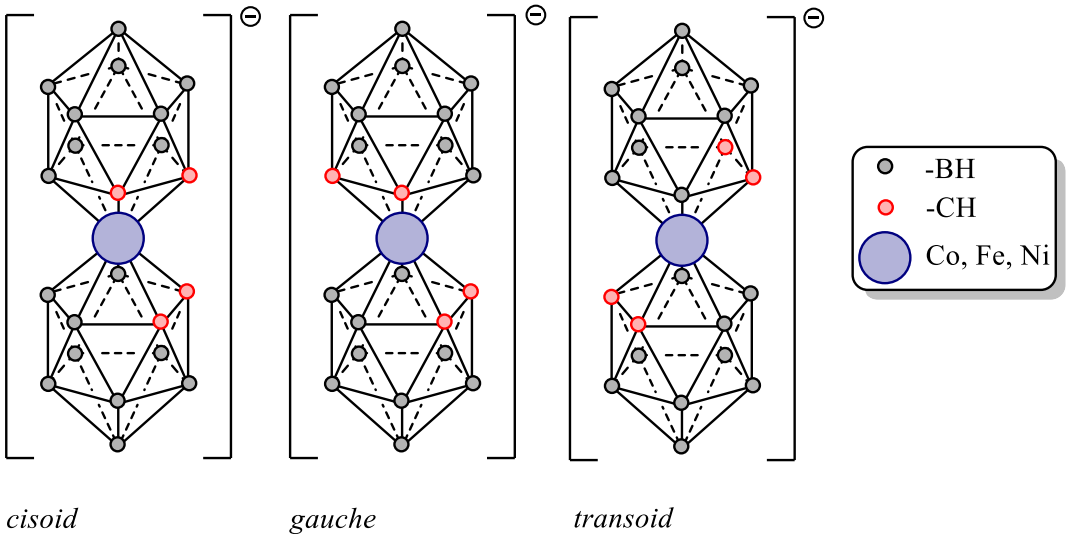

Figure 2.4 The structure of different rotamers of metalla-bis(1,2-dicarbollides).

2.2 Reactions of boron cluster compounds

2.2.1 Importance of the counterions and their exchange

Anionic boron cluster compounds form a variety of salts. Counterion plays a vital role in solubility[31, 32], reactivity[33], or in the solution behaviour of the clusters.[34, 35]

There are multiple ways to exchange the counterions. The first method is based on the precipitation of insoluble salts, e.g., tetraalkylammonium salts of *closo*-$[B_{12}H_{12}]^{2-}$ or caesium salt of COSAN. Another way, used chiefly for metallacarboranes, is extraction in the ether phase, designed by Plešek.[36] Nowadays, counterion exchange by ion-exchange chromatography is often used, where the stationary phase is modified cellulose or macroporous polymeric resins with incorporated strongly acidic sulphonic acid groups.

2.2.2 Modification of the framework of the boron clusters

2.2.2.1 Modification of B-H bond

In case of *closo*-dodecaborate anion (2-), all vertexes are equivalent due to symmetry, and mainly monosubstituted or persubstituted derivatives of boranes are known. Primarily used are derivatives containing bond boron-halogen, boron-sulphur, or boron-oxygen. Due to the aromatic nature of most boron cluster compounds, their chemistry is predominantly characterised by aromatic substitution reactions.

By the reaction of *closo*-$[B_{12}H_{12}]^{2-}$ anion with chlorine and bromine, $[B_{12}H_{12-n}X_n]^{2-}$ (n = 1 - 12) is formed. The rate of halogenation depends on the count of substituted vertexes and decreases with an increased number of substituted halogen atoms. Also, the rate decreases for different halogen atoms (Cl > Br > I). The persubstituted fluoro- and iodo-derivatives cannot be directly synthesised by the reaction with the respective element because the substitution reaction takes place only to a certain degree, and other procedures must be used. [37, 38, 39]

The derivatives with the boron-sulphur bond are nowadays mainly studied due to their potential use as a boron agent in BNCT cancer therapy (chapter 2.3.1.1). The mercapto derivatives could be prepared in multiple ways. The first synthetic procedure was based on the reaction of $(H_3O)_2[B_{12}H_{12}]\cdot nH_2O$ with hydrogen sulphide.[40] However, this reaction does not provide a high yield. Later other procedures, based on the reaction of closo-$[B_{12}H_{12}]^{2-}$ with thiocarbonyl compounds in an acidic solution, followed by hydrolysis in

the basic conditions.[41] Another option is the reaction of *closo*-$[B_{12}H_{12}]^{2-}$ with thiourea by electrochemical oxidation could prepare the respective mercapto derivatives.[42]

The perhydroxylated derivative of *closo*-$[B_{12}H_{12}]^{2-}$, $[B_{12}(OH)_{12}]^{2-}$, is prepared by refluxing with hydrogen peroxide.[43] The monohydroxylated derivative, $[B_{12}H_{11}(OH)]^{2-}$, can be prepared by reacting with amides in the acidic conditions followed by hydrolysis in the basic condition.[40] These compounds could be used to prepare a series of other derivatives; for example, we can obtain alkoxy derivatives, $[B_{12}H_{11}OR]^{2-}$, by the alkylation reaction with alkyl halides in the proper conditions[44, 45], or by the reaction with inorganic or organic acid dichlorides in acetonitrile, we can prepare bridged bis-cluster compounds.[46]

Oxonium derivatives of the polyhedral boron cluster compounds open other ways to prepare a broad range of functionalised compounds with various properties and applications.

As mentioned in chapter 2.1.1.3, polyhedral boron hydrides are commonly viewed as three-dimensional aromatic systems. Substitution reactions in these systems likely follow the mechanism of electrophilic aromatic substitution. However, due to the hydride character of hydrogen atoms in polyhedral boron hydrides, another mechanism may exist electrophile-induced nucleophilic substitution (EINS). This mechanism involves the primary attack of an electrophilic agent, eliminating hydride and electrophile to create a carbocation-like centre on the boron atom, which is then susceptible to the attack of a nucleophilic species. Many substitution reactions can occur by these two competitive mechanisms, resulting in mixtures of products from electrophilic and nucleophilic substitution. To prevent the formation of electrophilic substitution products, Lewis or Brønsted acids can be used. In the case of Brønsted acids, the electrophilic substitution mechanism leads to pure proton-proton exchange, while the nucleophilic substitution proceeds through dihydrogen molecule elimination. This mechanism is called acid-assisted nucleophilic substitution (AANS), which can be considered a specific case of the EINS mechanism. In the case of Lewis acids, simple abstraction of the hydride hydrogen atom by the acid takes place, resulting in a quasi-carbocation particle.[47] The mechanism of the substitution reaction is shown in Figure 2.5. In the case of using cyclic ether, e.g.,

tetrahydrofuran or 1,4-dioxane, this could be subsequently opened by the reaction with a variety of nucleophiles, as shown in Figure 2.6.

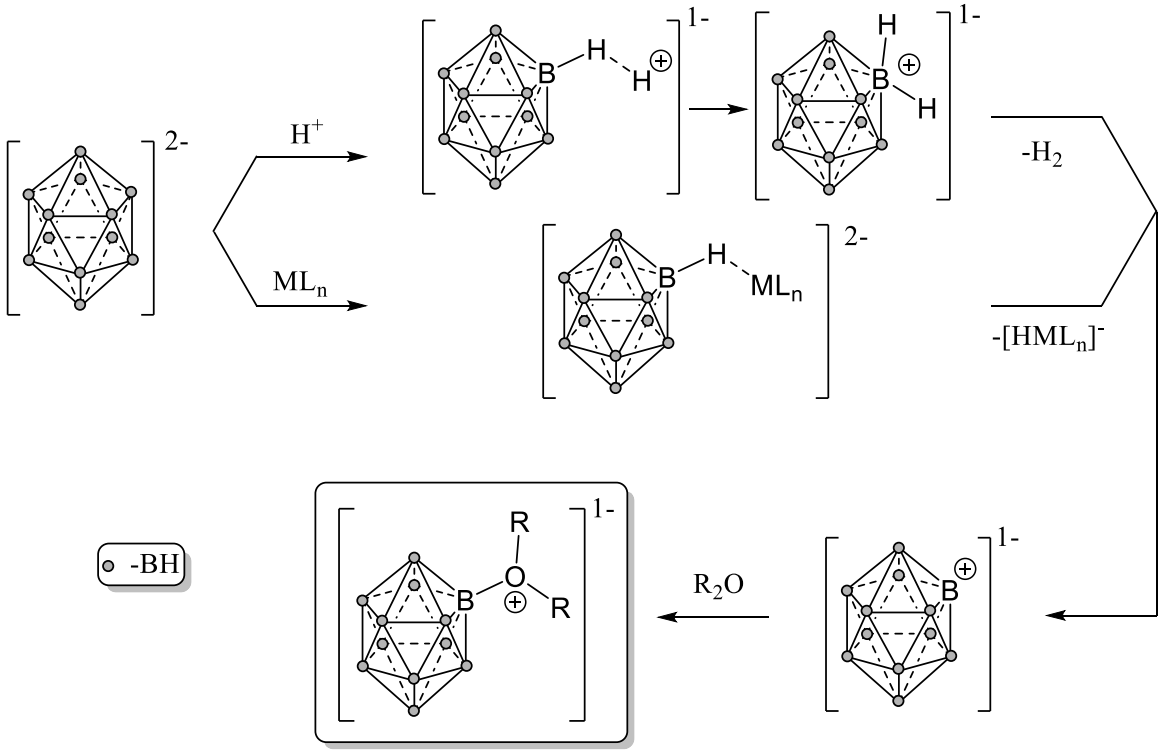

Figure 2.5 Mechanism of EINS reaction (adapted from ref [48]).

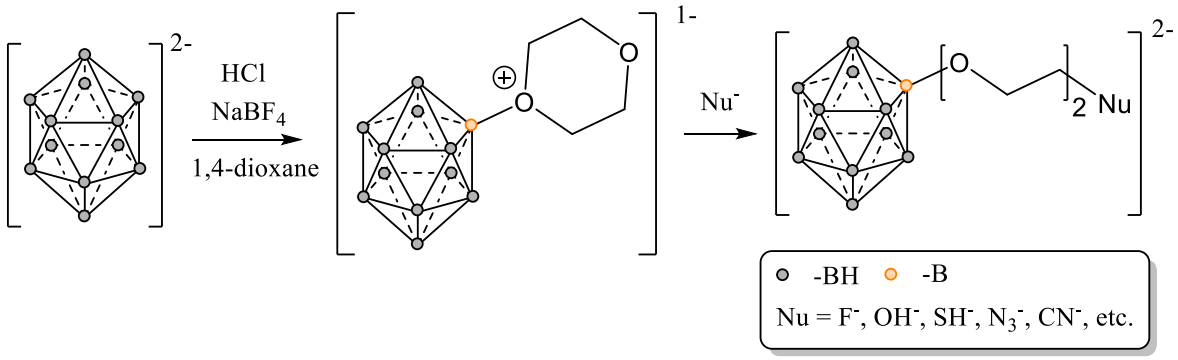

Figure 2.6 Ring-opening reaction of 1,4-dioxanate-*closo*-$[B_{12}H_{12}]^{2-}$ conjugate (adapted from ref [33, 47]).

When using diols in a ring-opening reaction, we can prepare a new type of amphiphile, so-called bola-amphiphiles. The term is derived from *bola*, a throwing weapon used to entangle an animal's legs, consisting of two or three balls of iron or stone fixed to the ends of a cord.[49] Thus, a hybrid compound composed of hydrophobic and hydrophilic

parts can be synthesised. Structure of *closo*-dodecaborate-based bola-amphiphile is shown in Figure 2.7.

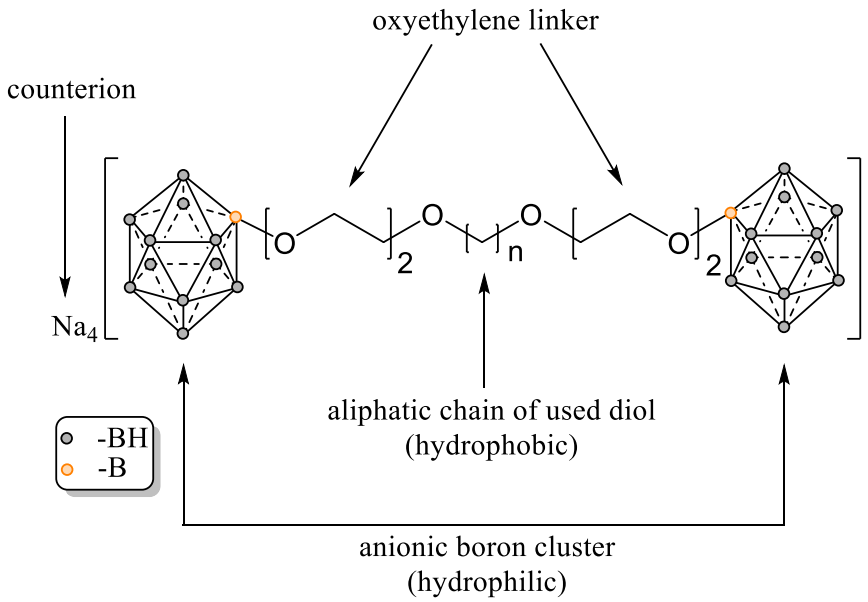

Figure 2.7 Structure of designed *closo*-dodecaborate-based bola-amphiphile.

In the case of carboranes and metallacarboranes, the [BH] vertexes are not equivalent, which is affected by the polarity of the [CH] group(s). This causes the reactivity of individual [BH] vertexes to depend on the spatial proximity from the [CH] fragment(s), as shown in Figure 2.8.

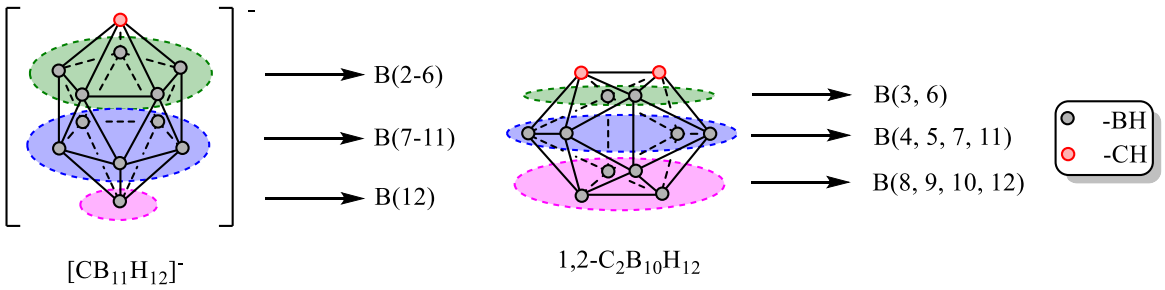

Figure 2.8 Spatial proximity of [BH] vertexes from [CH] fragment(s) in $[CB_{11}H_{12}]^-$ and 1,2-$C_2B_{10}H_{12}$. With respect to reactivity, the vertices are not equivalent and the reactivity decreases in the order of pink-blue-green marked [BH] fragments.

In the case of $[CB_{11}H_{12}]^-$, the reaction rate decreases in order: B(12) > B(7-11) > B(2-6). This is due to the increase of the electron density at B(12).[50] For the 1,2-$C_2B_{10}H_{12}$, the reaction rate is in order: B(8, 9, 10, 12) > B(4, 5, 7, 11) > B(3, 6). Also, catalysis by transition metals is used for the selective activation of [BH] fragments.[51]

Modifying the B-H bond in metallacarboranes is mainly performed on the B(8), respectively B(8'). This is opposite to both carbon atoms in the η^5 ligand ring. The reason for that is the highest electron density and easy activation by Lewis acid in this position.[6]

2.2.2.2 Modification of C-H bond in carboranes and metallacarboranes

Carboranes and metallacarboranes are more reactive species than boranes because of the weak acidic [CH] fragment. This can be deprotonated with strong nucleophilic species, e.g., butyllithium or Grignard reagent. It can subsequently react with a variety of electrophiles to prepare C-R derivatives (R = alkyl, aryl, halogen, carboxyl, hydroxyl, silyl, etc.).[6]

2.3 Applications of boron cluster compounds

2.3.1 Medical applications

Boron cluster compounds have been researched for their potential medical applications due to their unique chemical and physical properties, which allow polyhedral boranes to survive in many biological systems without degradation.

2.3.1.1 Boron neutron capture therapy (BNCT)

BNCT is a medical technique used to treat cancer. The principle of this procedure is the nuclear reaction of nonradioactive isotope ^{10}B with low-energy thermal neutrons to produce high-linear-energy transfer ions (alpha particles) that kill cancer cells with precision in the range of 5-9 μm. The nuclear reactions are shown in Figure 2.9. The key to success is the high accumulation (20-35 μg of ^{10}B per gram of tumour tissue is needed) and selective boron delivery into tumour tissue while minimising damage to surrounding healthy tissue. The ultimate goal is to destroy only tumour cells without harming healthy tissues in the irradiated area.[52]

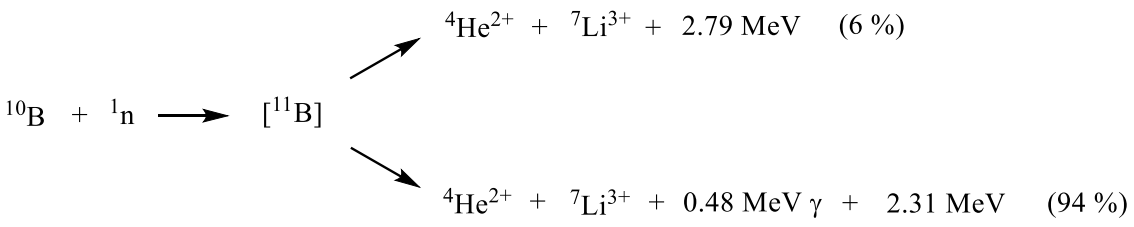

Figure 2.9 Nuclear reactions of ^{10}B with a low-energy thermal neutron (adapted from ref [52]).

Currently, two main boron containing compounds are approved by the U.S. Food and Drug Administration and thus used in BNCT: L-*p*-dihydroxyborylphenylalanine (BPA) and sodium mercaptododecaborate (BSH) (Figure 2.10) although these compounds have been used for more than 40 years for this purpose. The research, therefore, focuses on preparing derivates of boron cluster compounds, such as boronated saccharides[53], amino acids[54], nucleosides[55], liposomes[56], or porphyrins[57], with possible use in BNCT.

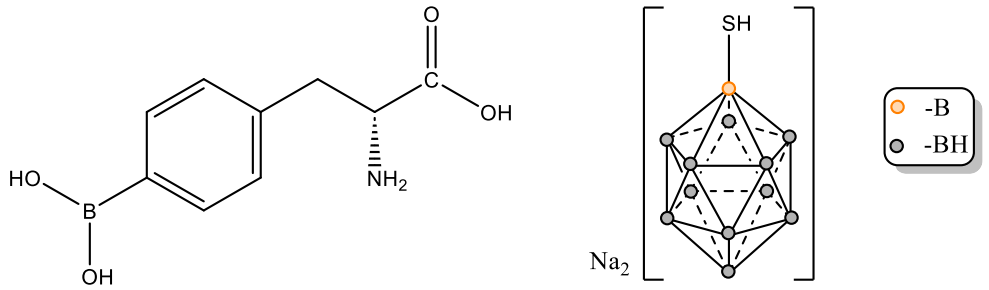

BPA BSH

Figure 2.10 Structures of used BNCT agents: L-*p*-dihydroxyborylphenylalanine (BPA) and sodium mercaptododecaborate (BSH).

2.3.1.2 Imaging

Another possible medical application of boron cluster compounds is in imaging. The biodistribution of the boron cluster can be monitored by using positron tomography, or single-photon emission computer tomography, depending on the used radionuclide incorporated. This is useful for the study of pharmacokinetics.[58] Later, a system containing carborane incorporated into the gadolinium complex used in magnetic resonance imaging was reported. The incorporation of carborane molecule caused slower metabolism of complex, compared to the mentioned complex on its own.[59]

Polyhedral boranes can also be used as X-ray contrast agents. Most contrast agents are composed of iodobenzene derivatives because of the opacity of the iodine atoms to low-energy X-rays.[60] Easy halogenation of boranes, resulting in molecules with a large number of iodine atoms per molecule, can be a way to prepare proper contrast agents.[61]

2.3.1.3 Antimicrobial properties

Boron cluster compounds possess antimicrobial properties and can be utilised in medicine. These compounds are not found in nature; hence, few biological systems can metabolise them. This makes them highly stable in these systems. Moreover, the

hydrophobic features of metallacarboranes, dicarboranes, and their derivatives allow them to penetrate the pathogen's lipid membrane without causing damage.[62, 63]

There are two ways in which the antimicrobial activity of these compounds occurs: first, by hindering the metabolic pathway crucial for the pathogen's survival, and second, by causing harm to the bacterial cell wall. Furthermore, derivatives of boron cluster compounds can also combat multidrug-resistant strains.

Apart from their antimicrobial activity, some boron cluster compounds can impede biofilm formation. This biofilm strengthens the pathogen's resistance to unfavourable environmental conditions or immune mechanisms, thus complicating the treatment process.[64]

2.3.1.4 Inhibitors of HIV Protease

The human immunodeficiency virus, or HIV, is an RNA virus that causes acquired immune deficiency syndrome (AIDS). To create infectious viral particles, the virus relies on protease. Drugs that inhibit the protease, called protease inhibitors, are commonly used to treat HIV. However, a significant challenge with HIV treatment is the virus's high resistance to these drugs. It was discovered that COSAN and its derivatives could act as specific inhibitors of HIV-1 protease. By binding to the hydrophobic pockets of sidechain residues of HIV protease, two COSANs anions can competitively inhibit the protease. Exoskeletal derivatives of metallacarboranes, shown in Figure 2.11 can further improve the effectiveness and selectivity of inhibition by other noncovalent interactions.[65, 66]

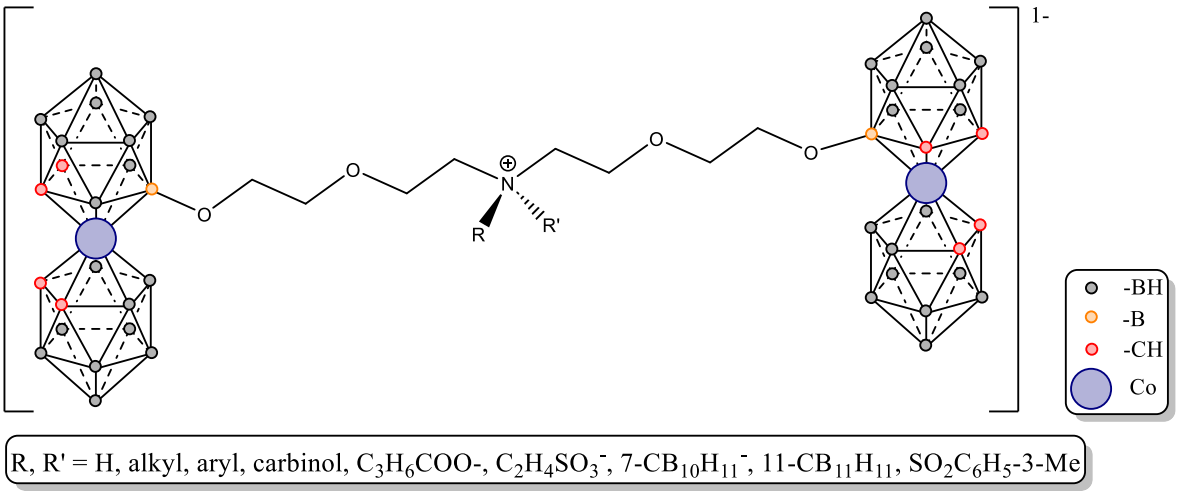

Figure 2.11 Structure of inhibitors of HIV protease derived from COSAN anion.

2.3.2 Material science

2.3.2.1 Liquid crystals

Liquid crystals, also called mesogens, are materials that behave as fluid at room temperature but have ordered structures. Nowadays, they are used, for example, in electro-optical displays. Because of their chemical properties, like chemical stability, cage-like design, or σ-aromaticity, are boranes and carboranes proper candidates for preparing liquid crystals in combination with organic rings. Examples of polyhedral borane-based molecules used as liquid crystals are shown in Figure 2.12.[67]

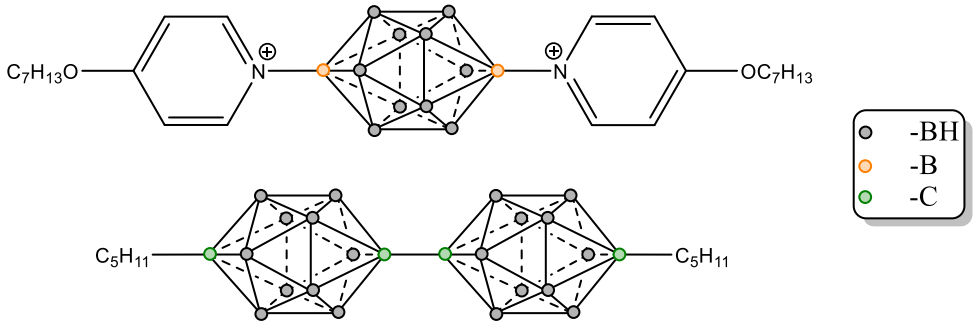

Figure 2.12 Structures of polyhedral boron clusters derivatives used as liquid crystals' materials.

2.3.2.2 Nonlinear optics

Nonlinear optics deals with the behaviour of the light in the media, where the polarisation density responds non-linearly to the electric field of a light wave. Materials with such properties are interesting for developing data storage, optical switches or protecting optical sensors from laser beams. It was shown that incorporating polyhedral boranes, as shown in the Figure 2.13, can increase the hyperpolarizability and thus improve the properties of the used material.[68]

2.3.2.3 Materials for ionic batteries

Another field of use of boron cluster compounds can be found in the development of materials for ionic batteries in electric cars and portable devices. COSAN is a weakly coordinating anion due to its low density of charge. This property is essential in this field of study. Firstly, COSAN has to be attached to the polymer chain, and afterwards, the delocalisation of the charge causes a decrease in the energy required for the migration of the counterion. One example of such an electrolyte is a derivative of COSAN-dioxanate conjugate, prepared by the reaction with 5-norbornene-2-methanol. Subsequently, norbornene is polymerised by metathesis polymerisation. Next, the prepared

poly(norbornene) is mixed with poly(oxyethylene), which causes the formation of a composite, where almost unlimited lithium (counterion) migration is observed.[69]

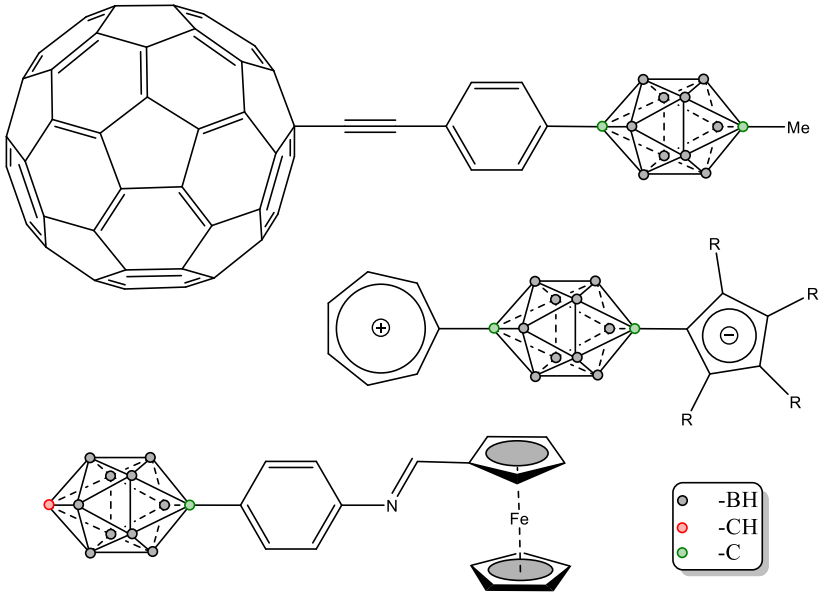

Figure 2.13 Carborane derivatives suitable for nonlinear optics materials.

2.3.2.4 Extraction of radionuclides

When processed, nuclear fuel generates liquid waste that contains radionuclides with long half-lives. To remove these radionuclides from the waste, COSAN is utilised because it transfers quantitatively from the aqueous phase to the organic phase. The solubility of COSAN in both phases results from the hydride character of hydrogen atoms on the BH groups due to charge delocalisation throughout the cage structure. The extraction process occurs in 3M HNO_3. Because of that, its derivatives, as shown in the Figure 2.14, are used instead, since COSAN is unstable under these conditions. These derivatives replace some of the hydrogen atoms on the boron atoms with halogen, methyl, or phenyl groups.

This extraction method can also be used to obtain cations of groups 1 and 2 of the periodic table and cations of lead, zinc, and silver, as well as lanthanides and actinoids. To improve the efficiency of extraction, crown ethers or other complexing agents are used along with the COSAN derivatives mentioned above.[70, 71] Also, for the extraction of ^{241}Am and ^{152}Eu radionuclides, *closo*-$[B_{12}H_{12}]^{2-}$ based derivatives were reported.[72]

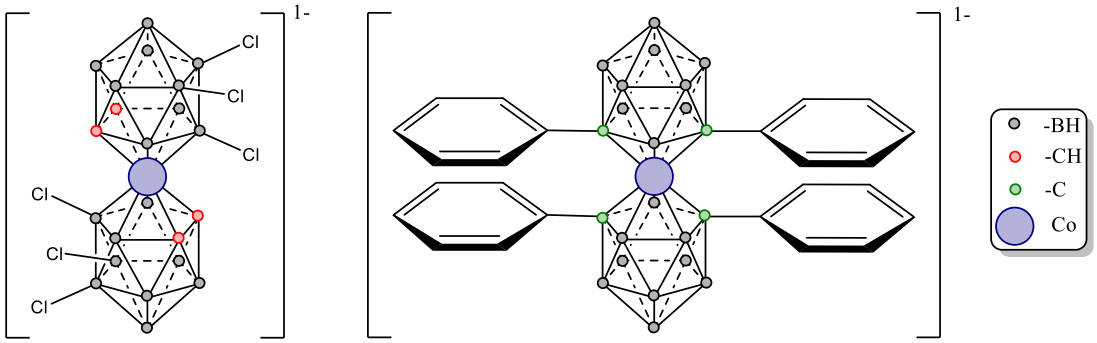

Figure 2.14 Structures of COSAN derivatives used in metal ion extraction applications.

2.3.3 Catalysis

Polyhedral boranes, as shown in the Figure 2.15, can also be used in catalysis. The hydridorhodium complex of dicarboranes can be used for the hydrogenation, hydroformylation and hydrosilylation of alkenes and alkynes. Similar results could be achieved using a fluorinated analogue of the mentioned hydridorhodium complex.[73] Nido-clusters can replace cyclopentadienyl anions in sandwich complex catalysts that hydrogenate alkynes to *cis*-alkenes. Another application of nido-cluster and metallacarboranes-based catalysts is in the controlled radical polymerisation of styrene, butyl acrylate or norbornene.[74, 75]

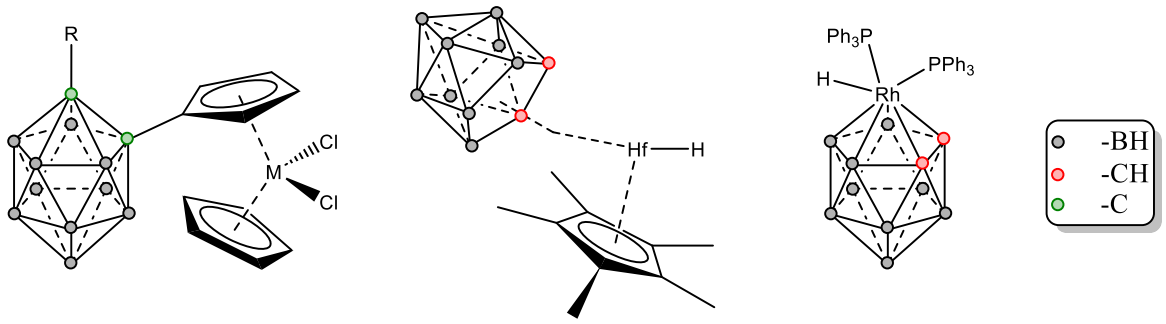

Figure 2.15 Structures of polyhedral borane catalyst precursors for the catalysis of hydrogenation, hydroformylation, hydrosilylation, or polymerisation reactions.

2.3.4 Perspective

Although considering the variety of possible uses of polyhedral boron cluster compounds discussed above, the main obstacle to bringing boron clusters to everyday applications is their high price. Recently, paper describing low cost, green and high yield synthesis of sodium or potassium salts of $[B_{10}H_{10}]^{2-}$ and $[B_{12}H_{12}]^{2-}$ via the reaction of sodium or potassium borohydride ($NaBH_4$, KBH_4) with borane-dimethyl sulphide complex in

autoclave.[76] In the case of metallacarboranes, prices of transition metals, mostly cobalt, are problematic. Even so there is effort to optimise the synthesis of metallacarboranes to reduce entry costs and so to lower the final price of metallacarboranes. For example, recent paper describes solvent-free synthesis of COSAN and its derivatives by the reaction of trimethylammonium dicarbollide with cobalt dichloride. This approach provides products in high yields and short reaction times.[77] Lowering the production costs and, thus, their prices could improve their unfulfilled potential for daily uses in the fields, where the properties of boron cluster compounds rapidly overwhelm other materials.

2.4 Boron cluster compounds as a building block in nano- and supramolecular chemistry

2.4.1 Self-assembly of boron cluster compounds

Self-assembly is a thermodynamically favourable process in which the spontaneous association of molecules into three-dimensional geometry under defined conditions. This approach is helpful in nanochemistry for the preparation of nanostructures.[78] Polyhedral boron cluster compounds were also investigated for their possible self-assembly behaviour. Micellization of metallacarboranes, such as COSAN, is an enthalpically driven process by a non-classical hydrophobic effect or a so-called chaotropic effect.[79] The term *chaotropic* (water-structure-breaking) describes the specific ion solvation and stems from the Hofmeister series. Chaotropic anions are large with low charge density. The opposite of chaotropes are *komsotropes* (water-structure-forming), small ions with a high charge density.[80] Some polyhedral boranes are also anions soluble in water; they can be included in the Hofmeister series, as shown in Figure 2.16. Dodecaborate anion and its derivatives are also called superchaotropes because they show a very strong chaotropic behaviour far beyond the scale of the Hofmeister series of ions.

Noncovalent interactions play a crucial role in the self-assembly of boron clusters because of terminal hydrogens with a negative partial charge. Because of that, they are weak hydrogen bond acceptors and donors. There are a few noncovalent interactions in boron clusters: *Weak hydrogen bonds*, which are weaker than classical hydrogen bonds and result from the interaction between a C-H hydrogen bond donor in carboranes and the electron density of aromatic molecules acting as a hydrogen bond acceptor. *Dihydrogen bonds* arise from the interaction between proton donors A-H, where A can be a carbon,

nitrogen, oxygen, or sulphur atom and the *σ*-bonding electron pair B-A, where B represents the boron atom. *σ-Hole bonding* occurs in the crystal packing of halogenated carboranes, and it is based on the interaction of halogen atoms with Lewis bases, which are electron donors.[81]

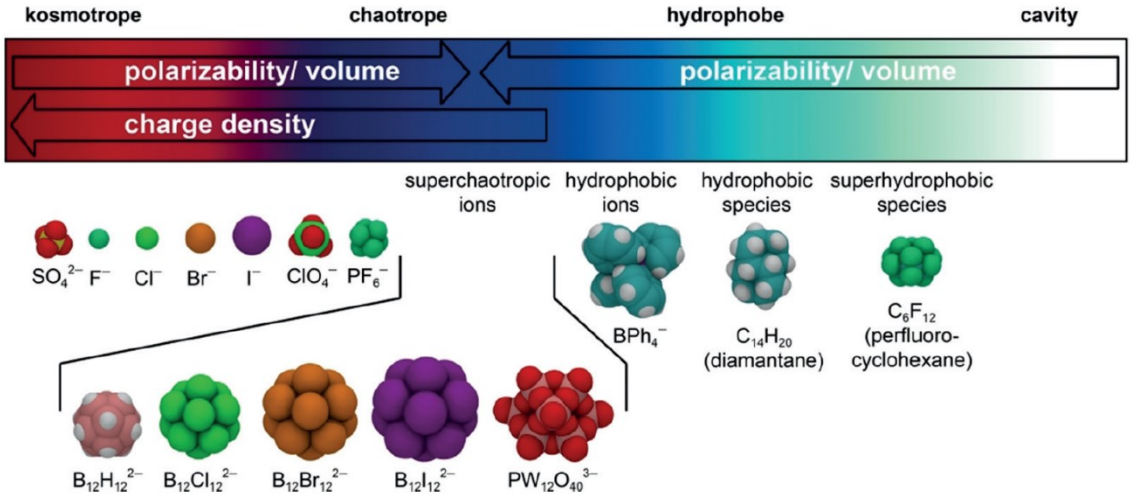

Figure 2.16 Extended Hofmeister series with included superchaotropes. Taken from the ref.[80]

2.4.2 Incorporation of boron cluster compounds into polymers

Polyhedral boron clusters can be incorporated with polymers by different approaches: by co-assembly of boron cluster compounds with polymer via noncovalent interactions mentioned previously, or by the inclusion of cluster as pendant group in sidechains or incorporated into polymer backbones. Concerning noncovalent interactions, the three most important properties are used as an approach to prepare nanostructures containing boron clusters: dihydrogen bonding[82, 83, 84], chaotropic effect[85] and electrostatic interactions.[86, 87, 88] Most polymers containing polyhedral boranes incorporated in their backbone include *o*-, *m*-, and *p*-carboranes and their derivatives. On the other hand, as a pendant group, *closo*-boranes, *o*-carborane or metallacarboranes and their derivatives are used.[6]

3 Characterisation techniques

3.1 Nuclear magnetic resonance (NMR) spectroscopy

Nuclear Magnetic Resonance (NMR) is an analytical technique based on the interaction of atomic nuclei with a non-zero nuclear spin in a magnetic field. Magnetic properties of nuclei are characterised by the nuclear angular momentum $\boldsymbol{I}$, which is proportional to the magnetic moment $\boldsymbol{\mu}$.

$$\boldsymbol{\mu} = \gamma \boldsymbol{I} \tag{3.1}$$

Where γ is the gyromagnetic ratio, a constant that characterises the given nucleus.

In the NMR, we can divide atomic nuclei into three groups: Nuclei with zero nuclear spin (e.g., ^{12}C, ^{16}O) do not possess any magnetic moment and thus are not observed in the NMR spectroscopy. Nuclei with spin ½ (e.g., ^{1}H, ^{13}C, ^{15}N, ^{19}F, or ^{31}P) possess magnetic moment and are easily measurable in the NMR. Nuclei with spin > ½ (e.g., ^{11}B, ^{17}O, or ^{27}Al) have, in addition to the magnetic moment, also an electric quadrupole moment, which is the reason for the more difficult NMR measurement of these nuclei.

The nuclear spin does not exhibit if the nucleus with the non-zero nuclear spin is not in a magnetic field. However, in the magnetic field $\boldsymbol{B}_0$, the result of the interaction of the magnetic field and the magnetic moment of the nuclei is a precessional motion of the vector of the magnetic moment $\boldsymbol{\mu}$ of the nucleus around the direction of $\boldsymbol{B}_0$. The frequency of this precession is expressed by the relation (3.2):

$$\nu = \frac{\gamma B_0}{2\pi} \tag{3.2}$$

where ν is the so-called Larmor frequency, and B_0 is the magnitude of the applied magnetic field $\boldsymbol{B}_0$.

A radiofrequency pulse must be used to measure the Larmor precession of the measured nuclei. It is generated by a magnetic field $\boldsymbol{B}_1$, whose vector is perpendicular to the $\boldsymbol{B}_0$. The resonance condition must be fulfilled (the frequency of the radiofrequency pulse is the same as the Larmor frequency of the measured nucleus). A macroscopic effect is observed after the resonance condition is met: the magnetisation vector begins to rotate around the $\boldsymbol{B}_1$. In NMR spectroscopy, 90- and 180-degree pulses are mainly used.

Because of relaxation processes, the magnetisation vector process to the original state by Larmor precession. Afterwards, a variable magnetic flux occurs in the coil generating $\boldsymbol{B}_1$. According to Ampere's law, the current is induced, a record of the NMR signal, also called free induction decay. This is subsequently processed by Fourier transformation to the NMR spectrum.

Electrons surrounding the nuclei interact with the $\boldsymbol{B}_0$ by creating an additional magnetic field, $\boldsymbol{B}_e$. As a result, the Larmor frequency is changed:

$$\nu = \frac{\gamma B}{2\pi} = \frac{\gamma}{2\pi}(B_0 - B_e) = \frac{\gamma}{2\pi}B_0(1-\sigma) \tag{3.3}$$

where σ is the so-called shielding constant. Various functional groups could be differentiated by the so-called chemical shift, defined as:

$$\delta = \frac{10^6(\nu - \nu_{ref})}{\nu_{ref}} \tag{3.4}$$

where δ is the chemical shift of the measured nucleus, ν is the Larmor frequency of the measured nucleus, and ν_{ref} is the Larmor frequency of the reference. For different nuclei, different references are used. In the ^1H and ^{13}C NMR spectroscopy, the chemical shift of respective atoms in tetramethylsilane ($SiMe_4$) is used as a reference. On the other hand, in ^{11}B NMR spectroscopy, the boron atom in the boron trifluoride etherate ($BF_3 \cdot Et_2O$) is used as a reference.[89, 90]

NMR spectroscopy could be utilised not only to determine the structure of chemical compounds. Diffusion-ordered spectroscopy (DOSY) is the pseudo-2D experiment resulting from pulsed field gradient spin or stimulated echo experiments and is used to determine diffusion coefficients. The principle of this method is based on measuring series a of pulsed field gradients stimulated echo spectra, in which the diffusion causes attenuation of NMR signal. The diffusion coefficient depends on the size and shape of the studied molecule; it also depends on the solvent's viscosity. For the spherical particles, we can use the calculated diffusion coefficient to determine the hydrodynamic radius (R_H) by adjusting the Stokes-Einstein equation (3.5):

$$D = \frac{k_B T}{6\pi\eta R_H} \tag{3.5}$$

where D is the diffusion coefficient, k_B is the Boltzmann constant, T is the thermodynamic temperature, and η is the solvent's viscosity. [90, 91]

3.2 Electrospray ionisation mass spectrometry (ESI-MS)

Electrospray ionisation (ESI) is a soft ionisation technique, because of little fragmentation. It belongs to atmospheric pressure ionisation and is suitable for analysing polar compounds with molecular weight in the magnitude of kDA to MDa. Because of that, it can also be used to analyse biopolymers.

ESI-MS begins with the sample being introduced into a chamber where it is dissolved in a suitable solvent, typically methanol or acetonitrile. The solution is then delivered through a capillary (nebuliser) tube to a high-voltage electrode, where it is subjected to a high electric field. This electric field causes the formation of tiny droplets at the tip of the capillary, which becomes charged due to the high voltage.

As the charged droplets move towards a counter electrode, they become smaller and smaller due to the evaporation of the solvent. Eventually, the droplets become so small that the surface tension is overcome, and a charged aerosol is formed. This aerosol contains tiny droplets containing one or more molecules from the original sample.

The charged aerosol is then introduced into a mass spectrometer, where it is directed towards an ionisation source. The charged droplets are further desolvated in the ionisation source and undergo gas-phase ionisation, forming gas-phase ions. This process involves the removal of one or more electrons from the molecule, resulting in the formation of a charged molecular ion.

The gas-phase ions are then separated by their m/z ratio using a mass analyser such as a quadrupole or time-of-flight analyser. The mass analyser allows the identification and quantification of the various ions in the sample based on their m/z ratio.[92, 93]

3.3 Light scattering (LS)

Scattering is a physical phenomenon in which the propagation of a radiation wave changes because of the interaction with matter. We can divide the scattering of radiation into three groups: elastic, where there is no energy exchange between radiation and matter (used in light scattering measurements). Inelastic scattering occurs when there is an excitation or deexcitation of matter by scattered radiation (for example, Raman scattering). Dynamic scattering occurs when scattered radiation changes due to the motions of matter. An example of dynamic (or quasi-elastic) scattering is the Doppler effect.

The mechanism of light scattering is based on the induction of the dipole moment by incident radiations that oscillate at the same frequency and act as a radiation source.

In static light scattering (SLS) measurements, we detect the angular dependence of the intensity of scattered light in the horizontal plane. The measured quantity is the Rayleigh ratio R defined by the relation 3.6:

$$R \equiv \frac{I_s r^2}{I_0} \tag{3.6}$$

where R is the Rayleigh ratio, I_s is the intensity of the scattered light related to the volume unit, r is the distance between the detector and the source of scattering (sample), and I_0 is the intensity of the light source (primarily lasers are used).

When the probability of a quantity fluctuation is expressed by changes in Helmholtz free energy and chemical potential μ, we get the relation for the Rayleigh ratio (3.7):

$$R = K(1 + \cos\theta)\, M_2 \phi_1 \frac{(k_B T)}{\left(\frac{\delta\mu}{\delta c}\right)} \tag{3.7}$$

where $K = [(4\pi^2 n_0^2)/(\lambda^4 N_A)]\,(\mathrm{d}n/\mathrm{d}c)^2$ is optical constant (contrast factor) λ is the wavelength, N_A is the Avogadro number, θ is the scattering angle, M_2 is the molar mass of the measured sample, ϕ_1 is the volume fraction of the solvent, k_B is the Boltzmann constant, and T is the thermodynamic temperature.

We can get the Zimm equation (3.8) from equation 3.7 by replacing the derivation of the chemical potential by virial expansion:

$$\frac{Kc}{R_\theta} = \frac{p^{-1}(\theta)}{M_2} + 2A_2c + \cdots \tag{3.8}$$

where A_2 is the second virial coefficient. From the static Zimm diagram, we can obtain the weight averaged molar mass $\langle M \rangle_w$, their radius of gyration R_g and the second virial coefficient A_2.

Dynamic light scattering (DLS) is based on correlation analysis of the time fluctuations of scattered light intensity resulting from interference of radiation scattered from randomly moving particles. The output of the measurement is a normalised intensity autocorrelation function $g^{(2)}(\tau)$ defined as:

$$g^{(2)}(\tau) = \frac{\int_o^\infty I(t+\tau)\ I(t)\ \mathrm{d}t}{\int_0^\infty I^2(t)\ \mathrm{d}t} \tag{3.9}$$

The intensity autocorrelation function is related to the electric field autocorrelation function $g^{(1)}(\tau)$ (3.10) by the Siegert relation (3.11):

$$g^{(1)}(\tau) = \exp(-\Gamma\tau) = \exp(-D^{\mathrm{eff}}q^2\tau) \tag{3.10}$$

$$g^{(2)}(\tau) = 1 - \beta\left(g^{(1)}(\tau)\right)^2 \tag{3.11}$$

where Γ is the relaxation rate proportional to the translational diffusion coefficient of the scattering particle, D^{eff} is the effective diffusion coefficient, and β is the deviation parameter from the ideal correlation. D^{eff} can be written as:

$$D^{\mathrm{eff}} = D(1 + CR_g^2q^2)(1 + k_Dc + \cdots) \tag{3.12}$$

$$D = \lim_{c,q\to 0} D^{\mathrm{eff}} \tag{3.13}$$

where D is the translational diffusion coefficient of the particles, C is the structure-dependent parameter, and k_D is the hydrodynamic virial coefficient. From the dynamic Zimm diagram, we can get the value of the diffusion coefficient (equation (3.13)), which can be used to calculate the hydrodynamic radius R_H after adjusting the Stokes-Einstein equation (3.5). [94, 95]

4 Materials and Methods

4.1 Chemicals

Sodium *closo*-dodecaborate (anhydrous, >98%) was purchased from Katchem. Tetra-*N*-butylammonium bromide (>99%), HCl (4M solution in dioxane), sodium hydride (60 wt%; suspension in mineral oil), sodium tetrafluoroborate (98%), caesium fluoride (99%) ethylene glycol (anhydrous, 99.8%), 1,4-butanediol (99%), 1,6-hexanediol (99%) 1,8-octanediol (98%), 1,10-decanediol (98%), 1,12-dodecanediol (99%), Amberlite® IR120 (H^+ form), Dowex® 50WX2 (200-400 mesh, H^+ form), Amberchrom® 50WX8 (200-400 mesh, H^+ form) and Dowex® 50WX8 (200-400 mesh, H^+ form) ion exchange resins were purchased from Sigma-Aldrich. 1,4-dioxane, tetrahydrofuran, and acetonitrile were purchased from Lach-ner. Dioxane and THF were purified according to the literature[96]; by drying over anhydrous calcium chloride overnight and distilling over sodium metal and benzophenone as an indicator in an argon atmosphere. After distillation, the solvents were stored in an inert atmosphere with molecular sieves 4A (Sigma-Aldrich). Acetonitrile was purified by stirring with phosphorous pentoxide for a few days and subsequent distillation. Subsequently, the solvent was stored with molecular sieves 4A. Other chemicals were used without further purification.

4.2 Polymer synthesis

Polymer samples of poly(ethylene oxide)-*block*-poly(2-(*N*, *N*, *N*', *N*'-tetramethyl guanidium ethyl acrylate), PEO_n-*b*-$PGEA_m$, were synthesised by Dr. Jianwei Li and Mgr. Soňa Mesíková, according to the literature.[87]

Shortly, in the first step, the macro chain transfer agent was synthesised by the reaction of 2-(((dodecylthio)carbonothioyl)thio)-2-methyl propanoic acid with methoxy poly(oxyethylene). The next step was the polymerisation of 2-bromoethyl acrylate by RAFT. Lastly, the synthesised polymer was functionalised by the reaction with 1,1,3,3-tetramethylguanidine. The synthetic route is shown in Figure 4.1. Three different polymer samples were prepared with different poly(acrylate) block lengths, shown in Table 4.1.

Table 4.1 Composition of prepared diblock copolymer samples

Polymer sample	*n*	*m*	M_n [$\cdot 10^3$ g·mol^{-1}] [1]	$Đ$ (M_w/M_n) [1]
P1	227	50	24.3	1.26
P2	227	80	32.8	1.25
P3	227	180	60.9	1.55

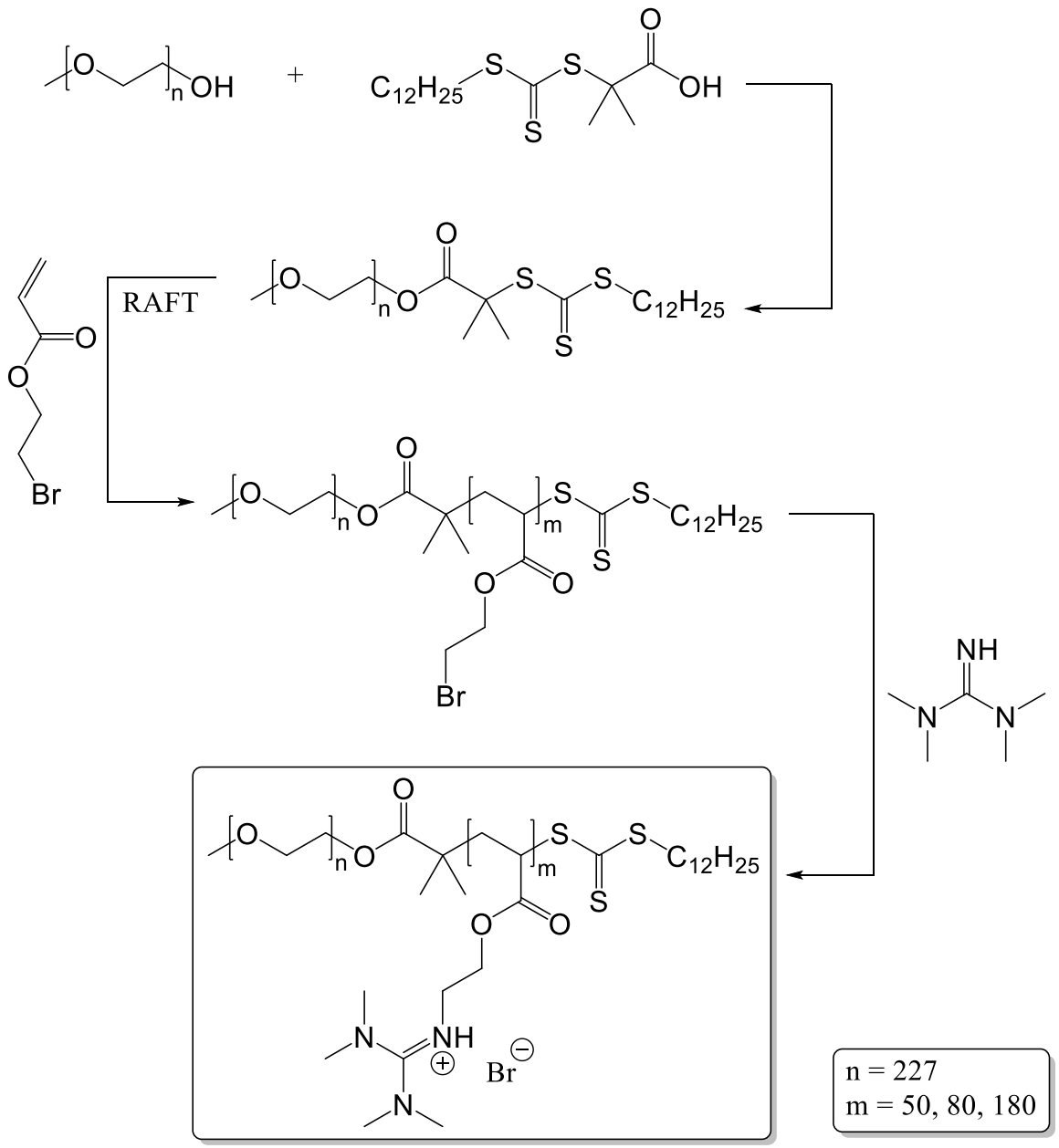

Figure 4.1 Synthetic steps of PEO_n-*b*-$PGEA_m$ copolymerisation.

[1] Values of M_n and $Đ$ were determined by size exclusion chromatography.

4.3 Methods

Nuclear magnetic resonance: Nuclear magnetic resonance (NMR) spectra were acquired on a Bruker Avance III HD spectrometer with decoupling accessories. The samples were dissolved in deuterated solvents (ARMAR AG, Sigma-Aldrich). The NMR spectra of ^{1}H and $^{1}H\{^{11}B\}$ (400.13 MHz), $^{13}C\{^{1}H\}$ (100.61 MHz) and $^{11}B\{^{1}H\}$ (128.38 MHz) were recorded. The proton NMR spectra were referenced to the residual solvent signal (4.79 ppm for water and 2.05 ppm for acetone). The chemical shifts are reported in parts per million (ppm) relative to the reference, and coupling constants are expressed in hertz (Hz). ^{1}H DOSY experiments were performed by Dr. Zdeněk Tošner on a Bruker Avance III operating at ^{1}H Larmor frequency of 600.17 MHz at 25 °C. Measurements were performed with the double-stimulated echo experiment using bipolar pulse field gradients [97] using 32 gradient values linearly spaced between 1 G/m and 49 G/m.

Mass spectrometry: Mass spectra were measured on a Bruker Esquire 3000 instrument using electrospray ionisation. Spectra were measured in negative mode. Samples were before measurements dissolved in HPLC grade acetonitrile.

Static and Dynamic light scattering: Static light scattering (SLS) and dynamic light scattering (DLS) were studied by using a light scattering photometer (ALV, Germany). The photometer consists of CGS-3 automatic goniometer, a 7004 multitau multibit autocorrelator, two high-QE APD pseudo-cross-correlation detectors and a 105 mW, 660 nm diode-pumped solid-state laser. SLS and DLS were measured simultaneously at 20°C. The scattering angles considered ranged from 50° to 130°, with an angular increment step of 20°. The analysis of DLS data involved fitting the measured normalised intensity autocorrelation function $g^{(2)}(t)$. The distribution of relaxation times, $\tau A(\tau)$, was obtained by performing an inverse Laplace transform of $g^{(1)}(t)$ using a constrained regularisation algorithm (CONTIN). Effective hydrodynamic radii, $R_H(q, c)$, which depend on the angle and concentration, were determined by calculating the mean values of relaxation times $\tau_m(q, c)$, for individual diffusive modes using the Stokes-Einstein equation (3.5). To obtain accurate hydrodynamic radii, the values of $1/R_H$ needed to be extrapolated to a zero-scattering angle. Since the refractive index increment, dn/dc, is unknown for all the samples, the light scattering intensity extrapolated to zero scattering angle was used as a proportional measure of the molar mass of polymeric nanoparticles in such cases.

4.4 Preparation of polymeric nanoparticles

For the preparation of polymeric nanoparticles, polymer samples of PEO_n-*b*-$PGEA_m$ (P1, P2 and P3; composition of block copolymers is shown in Table 4.1., page 26) with boron cluster dumbbells **Na_4[3]**, **Na_4[6]** and **Na_4[8]** (more details in synthetic part of the thesis, Figure 5.1, page 30) were used. Nanoparticles were prepared as follows:

For the light scattering measurements, 2 mg of polymer sample was dissolved in 2 ml of water (HPLC grade) to obtain a polymer concentration of 1 g/l. The solution was filtered through a syringe filter when all polymer was dissolved. Afterwards, a 0.05 M boron cluster dumbbell solution was prepared by dissolving its proper amount in the same HPLC grade water; this solution was afterwards filtered through a syringe filter. Polymeric nanostructures were prepared by titration experiment: boron cluster dumbbell solution was added to polymer sample solution to obtain dumbbell/guanidinium ratios of 0.00, 0.05, 0.10, 0.15, 0.20, 0.25, 0.30, 0.35, 0.50, 0.70 and 1.00. After each addition of boron conjugate, static and dynamic light scattering was measured.

In the case of NMR measurements, 1 g of polymer was dissolved in 1 ml of deuterium oxide; after dissolving all polymer, 0.5 µl of *tert*-butanol was added as standard. Subsequently, 0.025 M solutions of boron cluster dumbbells in deuterium oxide were prepared. Polymeric nanostructures were prepared by the same procedure as in the case of light scattering experiments. After each addition of the boron cluster dumbbell, a ^1H NMR spectrum was acquired.

5 Results and Discussion

5.1 Synthesis of the boron cluster derivatives

Synthesis of tetra-*N*-butylammonium *closo*-dodecaborate [1]:

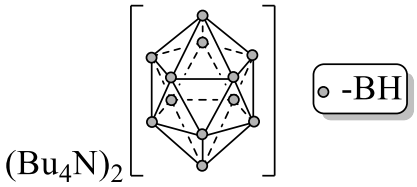

3 g (15.97 mmol) of sodium *closo*-dodecaborate was dissolved in 50 ml of distilled water. To this solution, 50 ml of tetra-*N*-butylammonium bromide water solution (10.81 g, 33.54 mmol) was added, forming a white precipitate, which was filtered, washed with water, and dried *in vacuo*. Yield: 9.343 g, 93%.

^{1}H{^{11}B} NMR (400.13 MHz, acetone-d6) δ 3.49 – 3.40 (m, 16H), 1.82 (m, 16H), 1.46 (h, J = 7.4 Hz, 16H), 1.26 (s, 12H), 1.00 (t, J = 7.4 Hz, 24H).

^{13}C{^{1}H} NMR (100.61 MHz, acetone-d6) δ 58.55, 23.67, 19.50, 13.06

^{11}B{^{1}H} NMR (128.38 MHz, acetone-d6) δ -15.21 (s)

Synthesis of the tetra-*N*-butylammonium 1,4-dioxanate-*closo*-dodecaborate conjugate [2]:

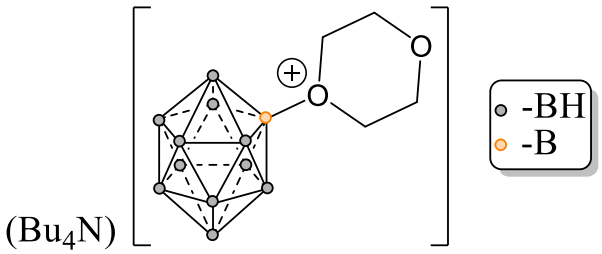

In the Schlenk flask with a stirrer, in an argon atmosphere, dry 1,4-dioxane (160 ml), **[1]** (4.00 g, 6.38 mmol), sodium tetrafluoroborate (3.50 g, 31.9 mmol) and hydrogen chloride solution in 1,4-dioxane (3.19 ml, 12.76 mmol) were added. The reaction mixture was refluxed in an argon atmosphere for 3 hours. After the reaction mixture was cooled to room temperature, it was filtered through a small piece of cotton and the liquid was evaporated. Yellowish oil left in the flask was dissolved in 20 ml of acetone. Subsequently, 30 ml of ethanol and 10 ml of water were added. After the addition of water, the yellow colour of the reaction mixture disappeared. The mixture was evaporated; after the evaporation of acetone, a white precipitate was observed. It was filtered, washed with a small amount of water and ethanol, and dried *in vacuo*—yield: 3.01 g, 79%.

^{1}H NMR (400.13 MHz, acetone-d6) δ 4.58 – 4.51 (m, 4H), 3.98 – 3.91 (m, 4H), 3.49 - 3.40 (m, 8H), 1.90 – 1.77 (m, 8H), 1.46 (h, J = 7.4 Hz, 8H), 1.00 (t, J = 7.3 Hz, 12H)

^{13}C{^{1}H} NMR (100.61 MHz, acetone-d6) δ 79.57, 64.85, 58.53, 23.57, 19.49, 12.99

^{11}B{^{1}H} NMR (128.38 MHz, acetone-d6) δ 9.05 (s), -17.11 (d, J = 124.7 Hz), -19.54 (s)

MS *m/z* (ESI^{-}) 229.3 (calc. 228.9) [M]$^{-}$

Synthesis of boron cluster dumbbells:

General procedure for the synthesis of boron cluster dumbbells is shown in Figure 5.1.

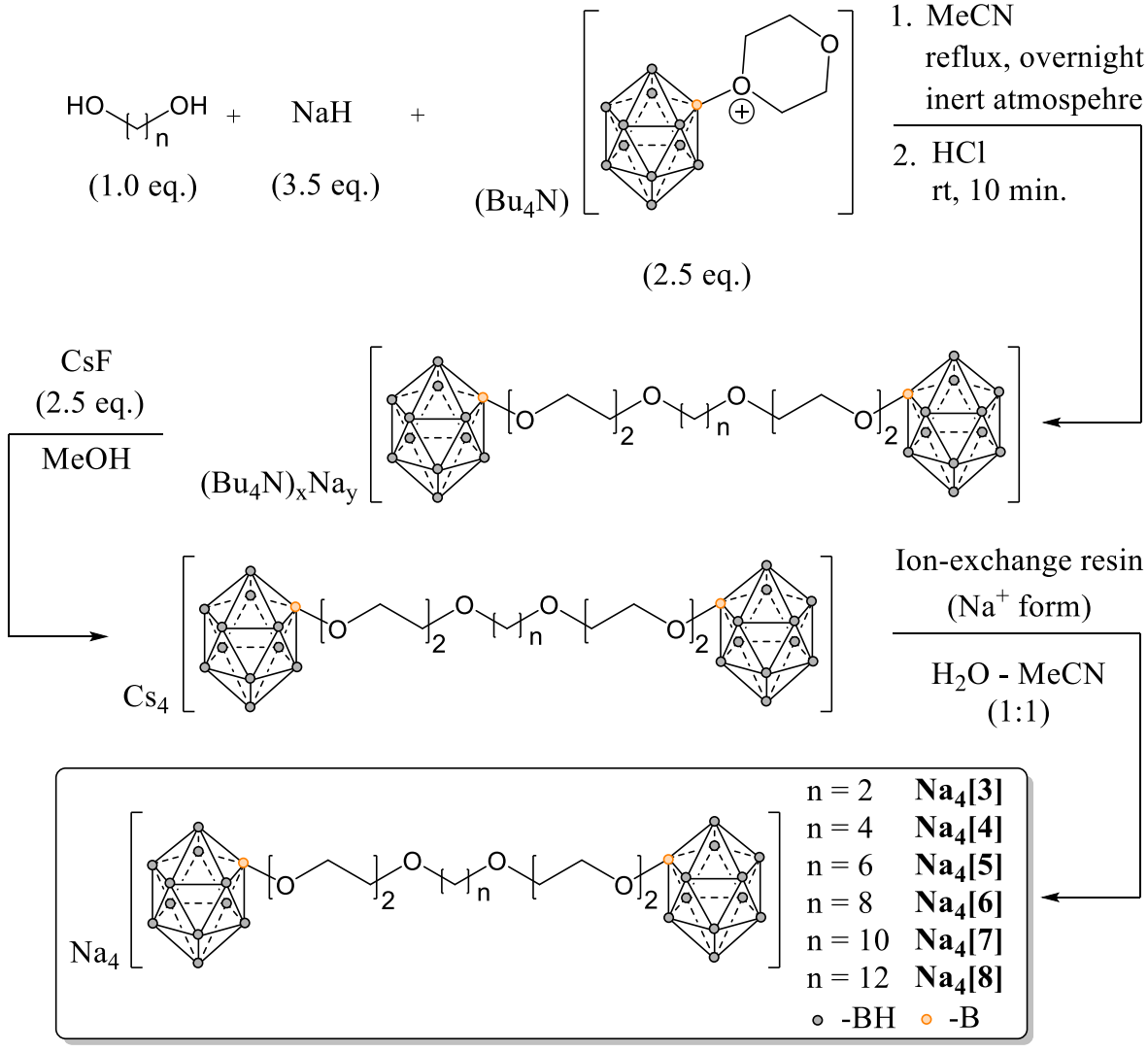

Figure 5.1 General procedure for the synthesis of boron cluster dumbbells.

Synthesis of **Na_4[3]**:

Ethylene glycol (16 mg, 0.254 mmol) was added to the round-bottom flask with a stirrer. Subsequently, the flask was flushed with nitrogen gas. Then dry acetonitrile (15 ml) was added, and after the dissolving of alcohol, sodium hydride (35 mg, 0.889 mmol) was added. The reaction mixture was stirred for 15 minutes until no hydrogen gas generation was observed. Next, in the reaction mixture, tetra-*N*-butylammonium 1,4-dioxanate-*closo*-dodecaborate conjugate **[2]** (300 mg, 0.636 mmol), dissolved in 5 ml of dry acetonitrile, was added. The reaction mixture was refluxed in a nitrogen atmosphere overnight. The next day, the reaction was quenched by adding a few drops of concentrated hydrochloric acid; afterwards, the mixture was filtered, and the liquid was evaporated to observe a yellow oil. This was dissolved in 10 ml of MeOH. To this solution, a caesium chloride (242 mg, 1.59 mmol) dissolved in methanol (1 ml) was added, causing the formation of a precipitate, which was filtered, washed with MeOH, and dried *in vacuo*. After drying, the solid was dissolved in a 5 ml H_2O-MeCN (1:1) mixture and added to the column with ion-exchange resin (Na^+ form). The solution was passed through the column at least three times. After that, the resin was filtered, and the liquid was evaporated and lyophilised.

^{1}H NMR (400.13 MHz, D_2O) δ 3.66 – 3.56 (m, 20H), 1.70 – 0.50 (bm, 22H).

^{11}B{^{1}H} NMR (128.38 MHz, D_2O) δ 6.55, -17.36 (d, J = 237.3 Hz), -23.27.

MS *m/z* (ESI$^-$) (MW 614.5) 591.4 (calc. 591.5) $[M + 3\ Na]^-$, 181.6 (calc. 181.8) $[M + Na]^{3-}$

Synthesis of **Na_4[4]**:

The same procedure as for the synthesis of **Na_4[3]** was used, but instead of ethylene glycol, 1,4-butanediol (23 mg, 0.254 mmol) was used.

^{1}H NMR (400.13 MHz, D_2O) δ 3.64 – 3.45 (m, 20H), 1.85 – 0.18 (bm, 26H).

MS *m/z* (ESI$^-$) (MW 642.5) 190.0 (calc. 191.2) $[M + Na]^{3-}$

Synthesis of **Na_4[5]**:

Following the synthetic steps for preparing **Na_4[3]**, but as a diol, 1,6-hexanediol (30 mg, 0.254 mmol) was used.

^{1}H NMR (400.13 MHz, D_2O) δ 3.68 – 3.41 (m, 20H), 1.89 – 0.16 (bm, 30H).

MS *m/z* (ESI$^-$) (MW 670.5) 645.5 (calc. 647.5) $[M + 3\ Na]^-$, 310.4 (calc. 312.28) $[M + 2\ Na]^{2-}$, 199.5 (calc. 200.5) $[M + Na]^{3-}$, 140.2 (calc. 144.7) $[M]^{4-}$

Synthesis of **Na_4[6]**:

The methodology employed to synthesise **Na_4[6]** was identical to **Na_4[3]**, except that instead of utilising ethylene glycol, 1,8-octanediol (37 mg, 0.254 mmol) was used.

^{1}H NMR (400.13 MHz, D_2O) δ 3.71 – 3.34 (m, 20H), 2.07 – 0.09 (bm, 34H).

MS *m/z* (ESI$^-$) (MW 698.6) 674.5 (calc. 675.5) $[M + 3\ Na]^-$, 324.3 (calc. 326.3) $[M + 2\ Na]^{2-}$, 210.4 (calc. 209.9) $[M + Na]^{3-}$

Synthesis of **Na_4[7]**:

By following the synthetic procedures outlined for the formation of **Na_4[3]**, 1,10-decanediol (44 mg, 0.254 mmol) was employed as the diol instead.

^{1}H NMR (400.13 MHz, D_2O) δ 3.65 – 3.43 (m, 20H), 2.09 – 0.09 (bm, 38H).

MS *m/z* (ESI$^-$) (MW 726.6) 220.3 (calc. 219.2) $[M + Na]^{3-}$, 157.3 (calc. 158.7) $[M]^{4-}$

Synthesis of **Na_4[8]**:

The synthetic steps for preparing **Na_4[3]** were followed, albeit substituting 1,12-dodecanediol (51 mg, 0.254 mmol) as the diol.

^{1}H NMR (400.13 MHz, D_2O) δ 3.81 – 3.35 (m, 20H), 1.96 – 0.07 (bm, 42H).

MS *m/z* (ESI$^-$) (MW 754.6) 352.3 (calc. 354.3) $[M + 2\ Na]^{2-}$, 226.7 (calc. 228.6) $[M + Na]^{3-}$, 165.4 (calc. 165.7) $[M]^{4-}$

Notes to the synthesis of boron cluster conjugates

Synthesis of 1,4-dioxanate-closo-dodecaborate conjugate **[2]**:

The priority is an anhydrous environment, as the presence of water could lead to the formation of an undesired by-product, resulting in lower reaction yield. Therefore, working using Schlenk equipment and a dry solvent is crucial. During solving of the project, two approaches were tried: drying 1,4-dioxane by overnight drying with $MgSO_4$, followed by distillation with sodium metal and benzophenone as an indicator, and subsequent storage in an inert atmosphere with activated molecular sieves (activated by drying in an oven for a few days at 150°C). The second method involved drying 1,4-dioxane directly with activated molecular sieves in an inert atmosphere. It was observed that higher yields were achieved with 1,4-dioxane dried by distillation.

In several cases, during the final synthesis step (dissolving the oil in acetone, ethanol, and water), the product did not precipitate after acetone evaporation. In most cases, complete evaporation and subsequent redissolution of the oil helped. However, there were occasions where only a small amount of product precipitated, which was filtered, and a portion of the resulting mother liquor was tested for crystallisation (using acetone as a solvent and cyclohexane as an antisolvent). This way, a part of the product was obtained as transparent crystals, but the yield was not high.

Synthesis of boron cluster dumbbells **[3-8]**:

Although the synthesis design is straightforward and functional for preparing similar compounds as reported in the paper [98], several problems arose during the solving of the project, requiring a significant amount of time for optimisation. These problems can be summarised into three categories: the occurrence and separation of product mixtures, the exchange of counterions in boron cluster conjugates, and reaction yields.

Multiple reaction products are possible during the reaction: the desired dumbbell, a monosubstituted conjugate of compound **[2]** and diol, or compound **[2]** with an open cycle. Monosubstituted conjugates may occur when an excess of diol is used. The solution is to employ a stoichiometric excess of conjugate **[2]** compared to the diol used. Additionally, it is necessary to use a stoichiometric excess of the sodium hydride since the concentration in the suspension cannot be accurately determined without analytical

methods such as titration. However, several risks are associated with this approach. The base, which does not react with alcohol to form alkoxides, reacts with compound **[2]**, resulting in the opening of the oxonium ring and the formation of an undesired side product. The presence of these side products was confirmed by NMR and MS, as shown in Figure 5.2 and Figure 5.3. From the NMR, it could be estimated that the synthetized samples contain ca. 85-90 mol.% of pure dumbbells **[3-8]** accompanied by a mixture of mentioned side-products. This is only approximately evaluation since some signals of desired and undesired products do overlap and thus the calculated integral values do not correspond correctly.

Another risk involves mineral oils in the sodium hydride suspension, which are challenging to separate from the products, likely due to their encapsulation in micelles formed by boron cluster conjugates. Purification of the product also requires optimisation. Water-organic solvent extraction is not desirable as it leads to product losses by washing a portion of it into the aqueous phase. Silica gel chromatography is complicated as compounds with high charge density, such as those being prepared, do not elute at all or exhibit tailing, making separating such a mixture impossible. Several conditions were tested, altering the composition of the mobile phase (DCM-MeOH, EtOAc-MeOH, MeCN), but none of the options resulted in sufficient product separation. Reverse-phase chromatography (mobile phase: MeCN-H_2O) was also attempted. The divided mixture was washed out in the initial fractions without successfully separating the product from impurities. A possible solution is to use ion-pairing high-performance liquid chromatographic separation [99], although it was not tested due to a lack of equipment.

Therefore, alternative purification methods were tried, in our case, the precipitation of boron clusters from the reaction mixture, since their solubility depends on the counterion, as mentioned in chapter 2.2.1. The oily product was dissolved in MeOH, and a solution of CsF in MeOH was added to form a precipitate, which was then filtered. However, this precipitate still contained impurities that needed to be removed. For this purpose, trituration was attempted using various solvents (MeOH, cyclohexane). With MeOH, a portion of the coloured impurities was washed out, but it was not entirely adequate; trituration with cyclohexane was not effective at all. Subsequently, recrystallisation was attempted. The procedure for synthesising similar compounds[98] (recrystallisation from hot water) was employed, but it did not lead to the precipitation of a pure product in this

case. Because of its relatively low boiling temperature, methanol was not used, so ethanol was utilised. Unfortunately, the product was not soluble in boiling ethanol; thus, another solvent must be used. The intermediate must be purified at this stage since purification becomes even more complicated after another counterion exchange step to get desired sodium salts.

Obtaining sodium salt from prepared boron cluster dumbbells is a multi-step process. Several approaches were performed.

The first approach consisted of an exchange to tetramethylammonium salt by dissolving the reaction mixture in the methanol-ethanol (1:1) mixture and adding the solution of tetramethylammonium chloride in the same mixture, resulting in a formation of a precipitate, which was filtered and dried *in vacuo*. Subsequently, the residue was dissolved in a water-acetonitrile (1:1) solution and was added to the column filled with the sodium form of ion-exchange resin. The solution was passed through the column multiple times. Afterwards, the solution was freeze-dried, and the sodium salt was obtained. This approach has its drawback; precipitated tetramethylammonium salt is also slightly soluble in methanol-ethanol solution, causing low reaction yields.

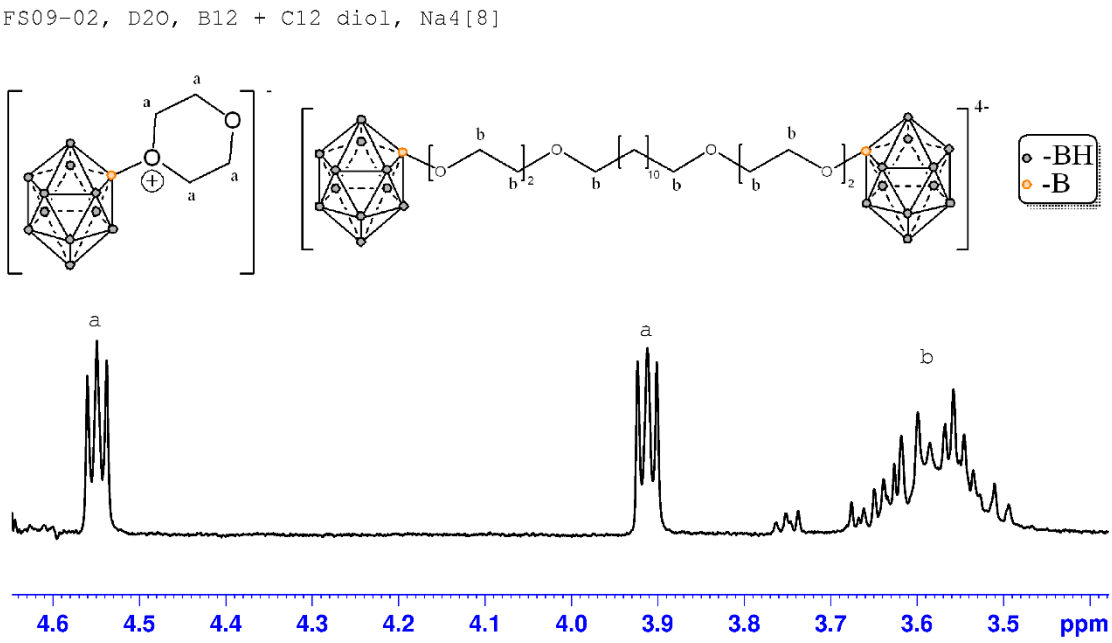

Figure 5.2 Part of the NMR spectrum of **Na_4[8]**, where a mixture of products can be observed; signals are assigned to the structures shown above the NMR spectrum. Signals *a* correspond to the hydrogens on the 1,4-dioxanate ring from the molecule **[2]**, signals *b* correspond to the hydrogens from the oxyethylene linker of **Na_4[8]**.

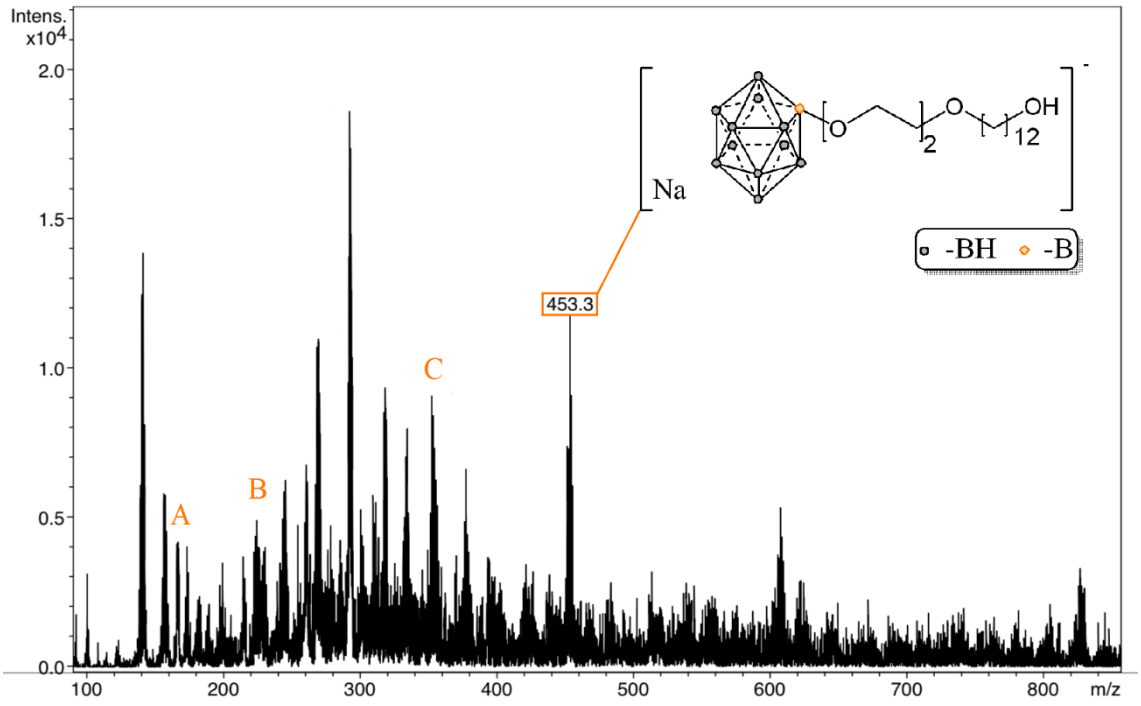

Figure 5.3 ESI$^-$ mass spectrum of **Na_4[8]**, where peak A represents $[M]^{4-}$ (m/z = 165.4), peak B is $[M + Na]^{3-}$ (m/z = 226.7) and peak C is $[M + 2\ Na]^{2-}$ (m/z = 325.3). Peak at m/z = 453.3 represents undesired product, which structure is shown.

The second approach was based on the precipitation of caesium salt and, subsequently, reaction with ion-exchange resin, as described above.

The third approach, used in synthesising other boron cluster conjugates, is based on the ion-exchange to the caesium salt and its purification. Afterwards, the precipitated product is dissolved in water, and a mixture of triethylamine and hydrochloric acid is added, which should lead to the formation of water-insoluble triethylammonium salt. This is subsequently dissolved in hot water, and a stoichiometric quantity of sodium hydroxide is added, which leads to the formation of desired sodium salt and water as a by-product. The solution is freeze-dried, and sodium salt is prepared. The most crucial step in this approach is to precisely add the stoichiometric amount of sodium hydroxide; in case of adding too much hydroxide, purifying sodium salt of boron conjugate and hydroxide will be impossible. In the case of the synthesis of boron cluster dumbbells, the problem was that the triethylammonium salt did not precipitate as expected. Because of that, the approaches using sodium form of ion-exchange resins were utilised. Multiple macroporous resins differed in their cross-linkage percentage, capacity, and particle size

were used. No significant difference in obtained yields for different resins used was observed. The only problem observed was that when the resin was kept stirring in a beaker for a few days, the lyophilizate was coloured the same colour as the used resin. Because of that, another method was used: the resin was filled into a chromatographic column, and the solution of boron cluster salt was passed through multiple times to be sure the ion-exchange did proceed. In that case, no colour contamination from the resin was observed.

As in detail described above, the synthesis of boron cluster dumbbells presented above provide meagre yields and purity of prepared products **[3-8]** (ca. 85-90 mol%), which is not sufficient for the self-assembly study of the dumbbells in water.[98] Nevertheless, these compounds were successfully used for the preparation of polymeric nanoparticles via co-assembly and the presence of anionic side-products did not deteriorate the formation of nanoparticles as described in chapter 5.2.

5.2 Characterisation of polymeric nanostructures

5.2.1 Static and dynamic light scattering

Static light scattering was used to track the formation of polymeric nanoparticles. After adding boron cluster dumbbells, angle-dependent light scattering intensity was measured and corresponding autocorrelation functions were collected. We can see the increase in the light scattering intensity, which is proportional to the molar mass of scatters, by a factor in order from 10 to 10^3. The saturation of nanoparticles by boron cluster dumbbells is observed at a 0.25 molar ratio of added boron cluster dumbbell (charge -4) to guanidium groups (charge +1) of the block copolymer, which is stoichiometrically expected to achieve electroneutrality. After further addition of boron cluster dumbbells, there is no increase in scattering intensity. The dependence of light scattering intensity to a molar ratio of **Na4[6]** to PEO$_n$-*b*-PGEA$_m$ is shown in Figure 5.4.

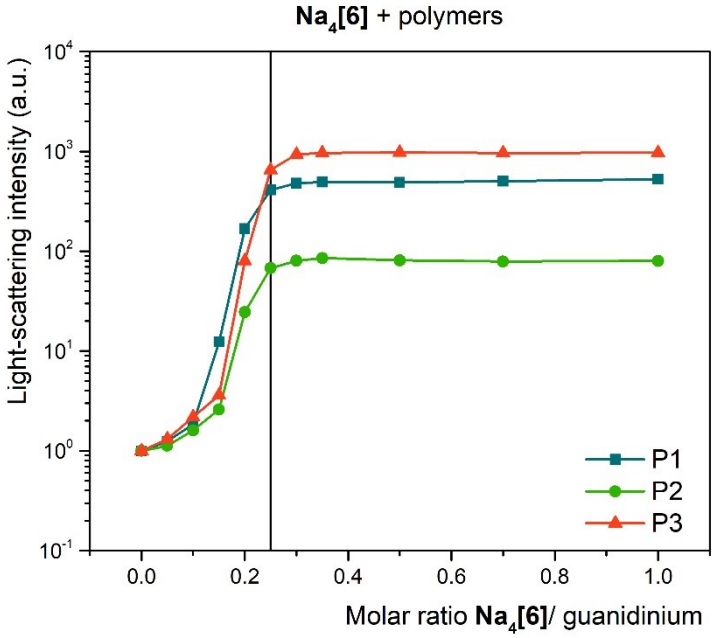

Figure 5.4 Dependence of light scattering intensity extrapolated to zero scattering angle to a molar ratio of added boron cluster dumbbell **Na4[6]** to polymer samples P1, P2, or P3. Polymeric nanostructures were prepared by the addition of the 0.05 M water solution of **Na4[6]** (structure shown in Figure 5.1, page 30) to PEO*n*-*b*-PGEA*m* block copolymers (P1, P2, or P3 respectively; composition of block copolymers is shown in Table 4.1., page 26) in water, to achieve molar ratio **Na4[6]**/ PEO$_n$-*b*-PGEA$_m$ from 0.00 to 1.00. The vertical line at 0.25 shows the ideal saturation point.

We can observe the increased value of hydrodynamic radii of prepared nanostructures after adding the boron cluster dumbbell from the dynamic light scattering measurements. Same as in the case of SLS measurements, there is no change after a 0.25 molar ratio of boron conjugates to block copolymers; thus, nanoparticles are saturated already.

Interestingly, there is a correlation related to the hydrodynamic radii of polymeric micelles. When using the same boron cluster dumbbell with different polymer samples, we can observe that the value of hydrodynamic radius decreases with a longer cationic block of the used block copolymer. Figure 5.5 shows a dependence in the value of hydrodynamic radii, R_H, on the length of a cationic block of used block copolymer, in the case of using **Na4[6]** conjugate.

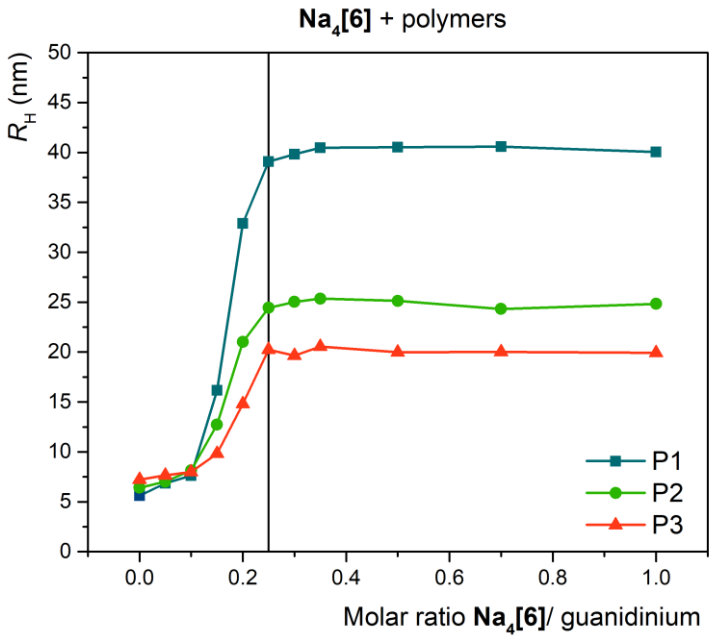

Figure 5.5 Dependence of hydrodynamic radius of nanoparticles to a molar ratio **Na4[6]**/ PEO$_n$-*b*-PGEA$_m$. Nanostructures were prepared by the addition of the 0.05 M water solution of **Na4[6]** (structure shown in Figure 5.1, page 30) to PEO*n*-*b*-PGEA*m* block copolymers (P1, P2, or P3 respectively; composition of block copolymers is shown in Table 4.1., page 26) in water, to achieve molar ratio **Na4[6]**/ PEO$_n$-*b*-PGEA$_m$ from 0.00 to 1.00. The vertical line at 0.25 shows the ideal saturation point.

To reveal the trend in changes of the hydrodynamic radii of nanoparticles prepared with different boron cluster conjugates, we carried out the constrained inverse Laplace transform routine, CONTIN, at 90° scattering angle for the most concentrated samples (molar ratio boron conjugate/ PEO$_n$-*b*-PGEA$_m$ = 1.00). All distributions shown in Figure 5.6 are monomodal and show that the value of the hydrodynamic radius of polymeric micelles decreases with longer cationic block and boron conjugate with longer aliphatic linker used. There is a noticeable difference in the values of R_H in the case of using **Na4[3]** and **Na4[6]** boron conjugates with different polymer samples. Just in the case of **Na4[8]**, this trend is not so evident because the values of R_H are almost identical for all prepared nanoparticles. It could be caused by lower possibilities of spatial arrangement because of the long aliphatic linker.

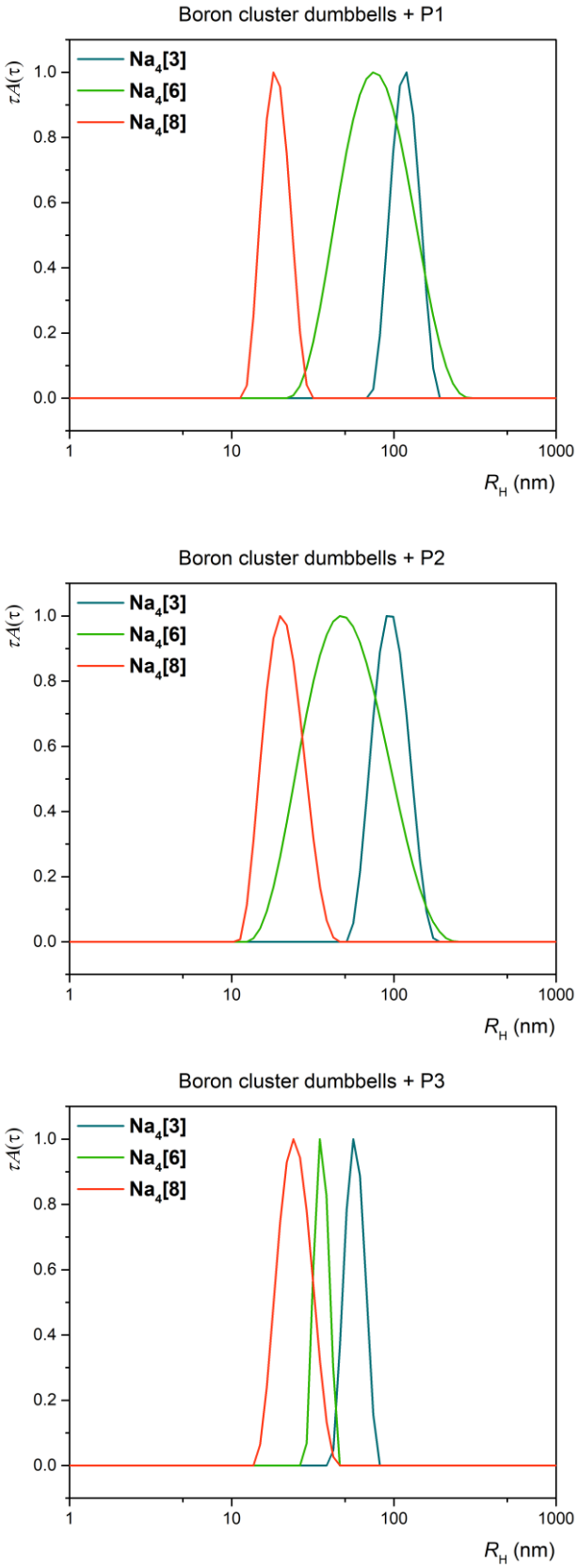

Figure 5.6 Hydrodynamic radii distribution of prepared polymeric nanoparticles resulted from CONTIN analysis of DLS autocorrelation functions at a 90° scattering angle. Nanoparticles were prepared by the addition of the 0.05 M water solution of **Na_4[3]**, **Na_4[6]** or **Na_4[8]** respectively **(**structures shown in Figure 5.1, page 30) to PEO*n*-*b*-PGEA*m* block copolymers (P1, P2, or P3 respectively; composition of block copolymers is shown in Table 4.1., page 26) in water. CONTIN analysis was performed for samples at molar ratio boron cluster dumbbell/ PEO*n*-*b*-PGEA*m* = 1.00.

5.2.2 Nuclear magnetic resonance spectroscopy

^{1}H NMR spectroscopy, similar to static light scattering, was used to study the formation of nanoparticles. During the addition of boron cluster dumbbells, we can see an attenuation of the signal of the polycationic block. Segments involved in the formation of the micelle core are observed more difficult or not at all in the NMR spectra. This happens because of decreased movement of polymer segments. In our case, the polycationic block reacts with boron clusters via noncovalent electrostatic interactions and thus, the movement of these segments is restricted, and the signal is attenuated.

Figure 5.7 shows measured ^{1}H NMR spectra of PEO_{227}-*b*-$PGEA_{50}$ during the addition of **Na_4[6]**. We can see that the signals of the linker of the used boron conjugate are visible only after the ideal saturation point, so all molecules of the conjugate added before that point were utilised for the formation of the nanoparticles and they are thus ‘’invisible’’. Also, the side-products from the dumbbell synthesis do not participate in the nanoparticle’s formation since their signal at 3.10 ppm is also observed before the ideal saturation point. In the case of the polycationic block, we can see that the signals of the cationic groups are narrower after the addition of the boron cluster dumbbell. Also, these signals are visible after nanoparticles are formed. This could mean that not every cationic segment is involved in the formation of nanoparticles. The fraction of frozen segments depends on the used polymer and boron dumbbell. Figure 5.8 shows a clear trend of increasing frozen polymer segments when using a longer polycationic block with the same boron conjugate. In the case of using different dumbbells with the same polymer, the trend is the same; hence the number of frozen polymer segments increases with larger boron conjugate used. The only deviation from this trend is observed in the case of nanoparticles formed by the longest polymer (P3) and the largest boron conjugate (**Na_4[8]**), and steric factors could cause it.

^{1}H DOSY NMR experiments were used to determine diffusion coefficients and thus to determine the hydrodynamic radii, R_H, of prepared nanoparticles. Since the diffusion coefficient determined from the DOSY measurements is number-averaged and depends on all compounds present in the sample, not only on the scatterers as in the case of the dynamic light scattering, the calculated values of R_H do not represent the correct values of hydrodynamic radii. Still, the relative meaning could be used for further interpretation. All calculated values of R_H were related to the value of the R_H of the nanoparticles formed

by P1 and **Na$_4$[3]**, which is assumed to have the highest value of the R_H, determined from the dynamic light scattering measurements. From Figure 5.9, it can be noted the same trend of the values of the hydrodynamic radii of prepared nanostructures as from the DLS measurements. Hence, the value of the R_H of the nanoparticles decreases with a longer cationic block and larger boron conjugate used in the polymeric nanostructure.

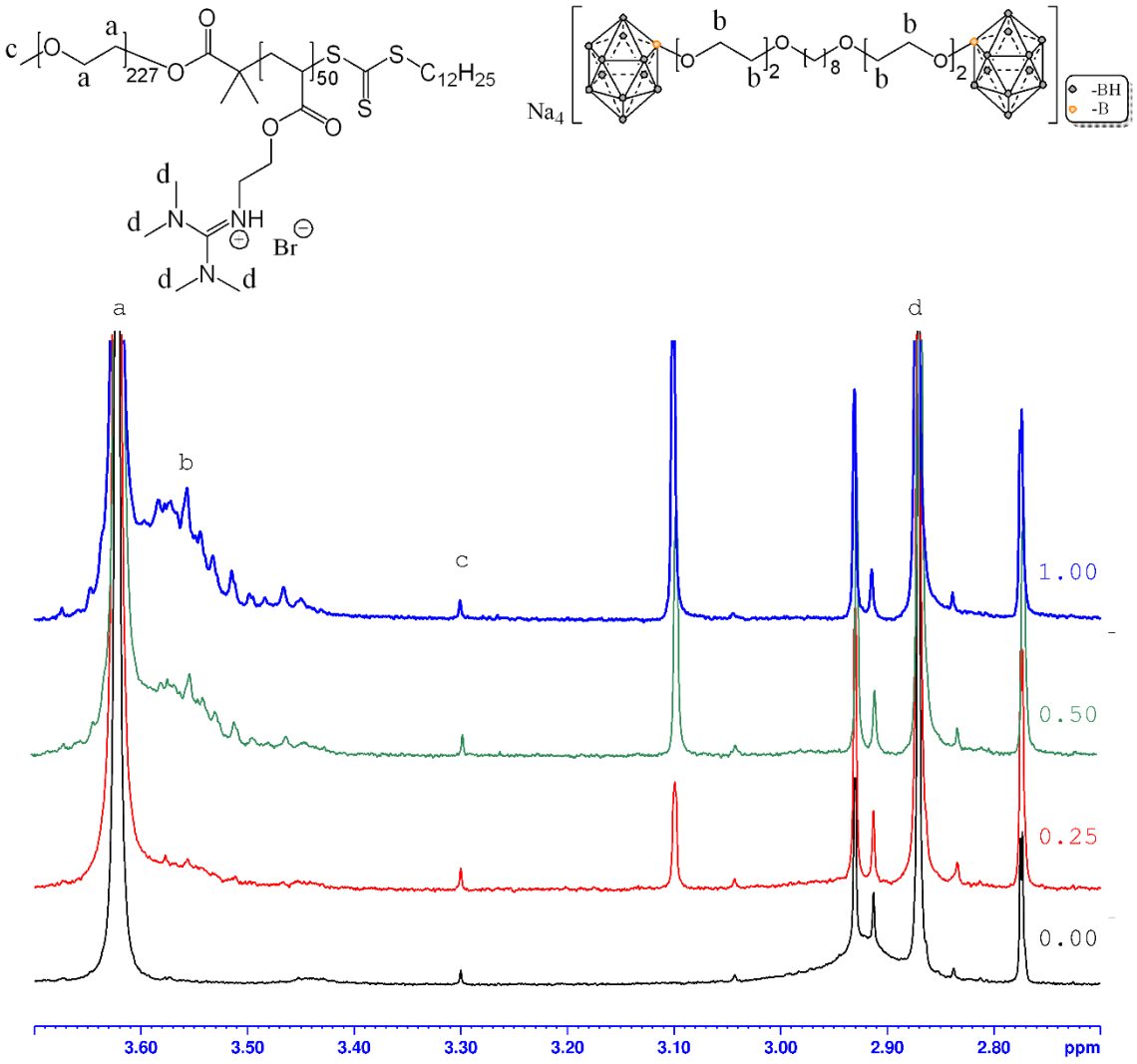

Figure 5.7 ^{1}H NMR spectra of PEO$_{227}$-*b*-PGEA$_{50}$ at different molar ratios **Na$_4$[6]**/ PEO$_{227}$-*b*-PGEA$_{50}$ (0.00, 0.25, 0.50 and 1.00). Polymeric nanoparticles were prepared by the addition of the 0.025 M deuterium oxide solution of **Na$_4$[6]** (structure shown in Figure 5.1, page 30) to PEO*n*-*b*-PGEA*m* block copolymers (P1, P2, or P3 respectively; composition of block copolymers is shown in Table 4.1., page 26) in deuterium oxide. Signals are assigned to the structures shown above the NMR spectra. Signal *a* corresponds to the hydrogens of PEO, signals *b* correspond to the hydrogens from the oxyethylene linker of **Na$_4$[6]**, signal *c* corresponds to the methyl end-group of PEO$_{227}$-*b*-PGEA$_{50}$ block copolymer and signals *d* correspond to the PGEA. Signal at approximately 3.10 ppm corresponds to the side-product from the synthesis of **Na$_4$[6]**.

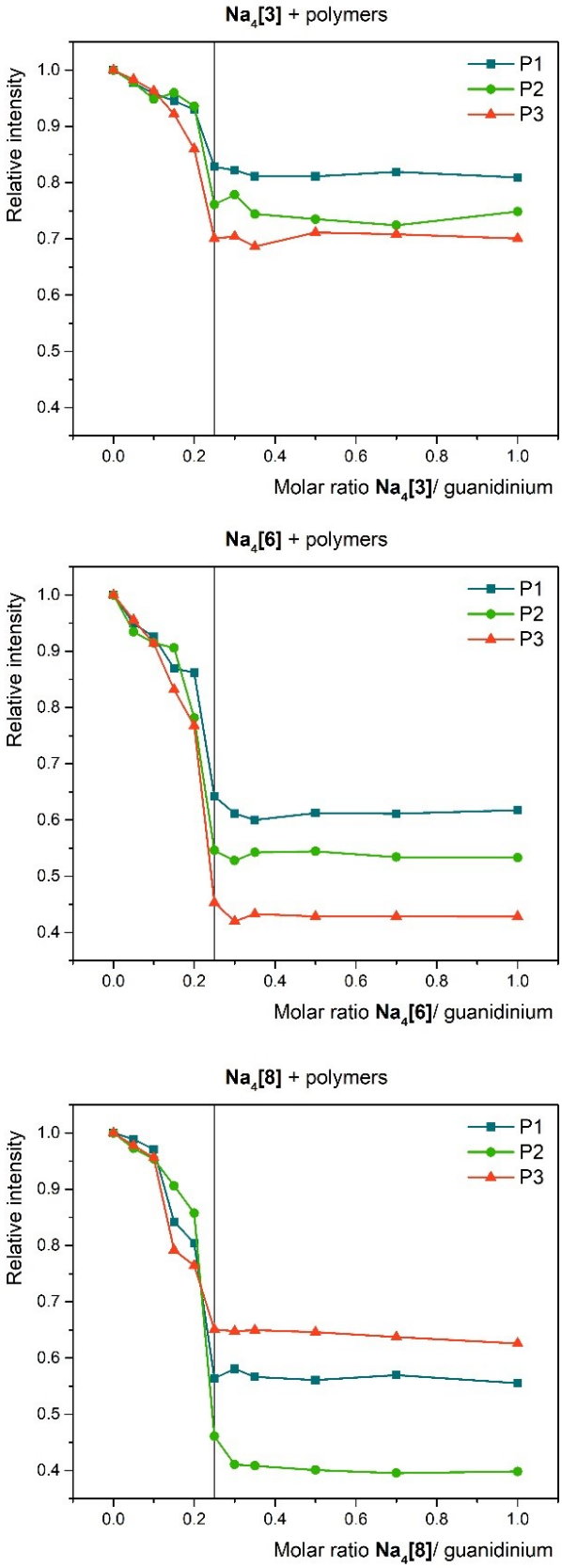

Figure 5.8 Relative intensity of ^{1}H NMR signal of PGEA block in prepared polymeric nanostructures. These were prepared by the addition of the 0.025 M deuterium oxide solution of **Na4[3]**, **Na4[6]** or **Na4[8]** respectively (structures shown in Figure 5.1, page 30) to PEO*n*-*b*-PGEA*m* block copolymers (P1, P2, or P3 respectively; composition of block copolymers is shown in Table 4.1., page 26) in deuterium oxide, to achieve molar ratio boron cluster dumbbell/ PEO_n-*b*-$PGEA_m$ from 0.00 to 1.00. The vertical line at 0.25 shows the ideal saturation point.

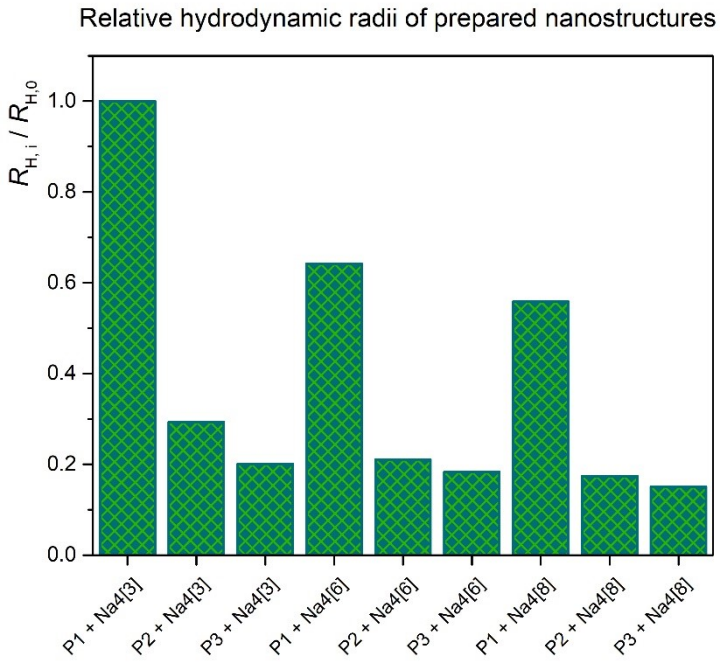

Figure 5.9 Relative hydrodynamic radii of prepared nanostructures resulted from ^{1}H DOSY analysis. Polymeric nanoparticles were prepared by the addition of the 0.025 M deuterium oxide solution of **Na_4[3]**, **Na_4[6]** or **Na_4[8]** respectively (structures shown in Figure 5.1, page 30) to PEO*n*-*b*-PGEA*m* block copolymers (P1, P2, or P3 respectively; composition of block copolymers is shown in Table 4.1., page 26) in deuterium oxide. All values of hydrodynamic radii, $R_{H,i}$, were related to the value $R_{H,0}$. The value of $R_{H,0}$ corresponds to the value of hydrodynamic radius of the nanostructure formed by the addition of deuterium oxide solution of **Na_4[3]** to the PEO_{227}-*b*-$PGEA_{50}$ (P1) in deuterium oxide. Hydrodynamic radii were estimated for samples at molar ratio boron cluster dumbbell/ PEO*n*-*b*-PGEA*m* = 1.00.

6 Conclusion

In summary, this diploma thesis was aimed at the preparation of nanostructures based on noncovalent electrostatic interactions of conjugates of the polyhedral *closo*-dodecaborate anion (2-), promising building blocks in nanochemistry, with cationic polyelectrolytes in water.

The boron cluster dumbbells were synthesised from the commercially available sodium salt of the *closo*-dodecaborate anion (2-), $Na_2[B_{12}H_{12}]$, by the exoskeletal, electrophile-induced nucleophilic substitution (EINS) and by subsequently ring-opening reaction with a variety of aliphatic diols, resulting in hybrid dumbbell molecule, consisted of hydrophilic anionic boron clusters, their counterions, and hydrophobic linker. Unfortunately, the synthesis resulted in a mixture of products with relatively low yield and purity ca. 85-90 mol%. With desired boron cluster dumbbell, also monosubstituted conjugate or unreacted reactant did occur in the reaction mixture. The problem was partially solved by adding stochiometric excess of the reactant and base used for the deprotonation of diol. Another problem was the purification of products, since the silica chromatography was not successful, because synthesised products did not elute, or exhibited tailing. The purest products were achieved after the precipitation of the salt with different counterion. Other problem occurred during the counterion exchange since some procedures did not work for prepared boron cluster dumbbells. This was solved by using ion-exchange resins. Despite the problems described above, synthesised compounds were found suitable for the preparation of well-defined polymeric nanostructures.

The polymeric nanoparticles were prepared by co-assembly of boron cluster dumbbells and poly(ethylene oxide)-*block*-poly(2-(*N*, *N*, *N*', *N*'-tetramethyl guanidium ethyl acrylate) (PEO_n-*b*-$PGEA_m$) diblock copolymers in water. The formation of nanoparticles and their hydrodynamic radii, R_H, were studied by static and dynamic light scattering and NMR spectroscopy.

The formation of nanoparticles was confirmed by static light scattering and ^{1}H NMR spectroscopy since increased light scattering intensity and decreased signal intensity in ^{1}H NMR spectra, respectively. Hydrodynamic radii of prepared nanostructures were studied by dynamic light scattering and ^{1}H DOSY NMR. Both techniques showed that the value of hydrodynamic radii is strongly dependent on the length of the polycationic

block and on the size of the aliphatic linker of the boron cluster dumbbell, so the value of hydrodynamic radius of the prepared nanostructure decreases with longer polycation and longer dumbbell used.

Despite many obstacles and difficulties while solving this project, the outcomes could be applied to further studies of supramolecular properties of boron cluster compounds, their derivatives, and their use in nanochemistry.

References

1. Housecroft, C. E. & Sharpe, A. G. *Inorganic chemistry*. (Pearson, 2012).

2. Housecroft, C. E. *Boranes and Metalloboranes: Structure, Bonding and Reactivity*. (Ellis Horwood ; John Wiley & Sons, 1990).

3. Stock, A. *Hydrides of Boron and Silicon.* (Cornell University Press, 1933).

4. Greenwood, N. N. Ludwig Mond Lecture. Taking stock: the astonishing development of boron hydride cluster chemistry. *Chemical Society Reviews* **21**, 49 (1992).

5. *Chemistry of the Elements*. (Elsevier, 1997). doi:10.1016/c2009-0-30414-6.

6. Grimes, R. N. *Carboranes*. *Carboranes* (Elsevier, 2016). doi:10.1016/c2014-0-01334-2.

7. Lipscomb, W. N. The boranes and their relatives. *Science* **196**, 1047–1055 (1977).

8. Dickerson, R. E. & Lipscomb, W. N. Semitopological approach to boron-hydride structures. *The Journal of Chemical Physics* **27**, 212–217 (1957).

9. Lipscomb, W. N. Recent Studies of the Boron Hydrides. in *Advances in Inorganic Chemistry and Radiochemistry* 117–156 (1959). doi:10.1016/S0065-2792(08)60253-8.

10. Wade, K. The structural significance of the number of skeletal bonding electron-pairs in carboranes, the higher boranes and borane anions, and various transition-metal carbonyl cluster compounds. *Journal of the Chemical Society D: Chemical Communications* 792–793 (1971) doi:10.1039/C29710000792.

11. Fox, M. A. & Wade, K. Evolving patterns in boron cluster chemistry. *Pure and Applied Chemistry* **75**, 1315–1323 (2003).

12. Mingos, D. M. P. & Wales, D. J. *Introduction to cluster chemistry*. (Prentice Hall, 1990).

13. Jemmis, E. D. & Jayasree, E. G. Analogies between Boron and Carbon. *Accounts of Chemical Research* **36**, 816–824 (2003).

14. Von Schleyer, P. R. & Najafian, K. Stability and Three-Dimensional Aromaticity of closo-Monocarbaborane Anions, CBn-1Hn-, and closo-Dicarboranes, C2Bn-2Hn. *Inorganic Chemistry* **37**, 3454–3470 (1998).

15. King, R. B. Three-Dimensional Aromaticity in Polyhedral Boranes and Related Molecules. *Chemical Reviews* **101**, 1119–1152 (2001).

16. Poater, J., Solà, M., Viñas, C. & Teixidor, F. π Aromaticity and Three-Dimensional Aromaticity: Two sides of the Same Coin? *Angewandte Chemie International Edition* **53**, 12191–12195 (2014).

17. Hoffmann, R. & Lipscomb, W. N. Theory of Polyhedral Molecules. I. Physical Factorizations of the Secular Equation. *The Journal of Chemical Physics* **36**, 2179 (1962).

18. Hoffmann, R. & Lipscomb, W. N. Theory of Polyhedral Molecules. III. Population Analyses and Reactivities for the Carboranes. *The Journal of Chemical Physics* **36**, 3489 (1962).

19. Hoffmann, R. & Lipscomb, W. N. Boron hydrides: LCAO-MO and resonance studies. *The Journal of Chemical Physics* **37**, 2872–2883 (1962).

20. Richard T. Holzmann, Hughes, R. L., Smith, I. C. & Lawless, E. W. *Production of the boranes and related research*. (1967).

21. González-Moraga, G. *Cluster Chemistry*. (Springer Berlin Heidelberg, 1993). doi:10.1007/978-3-642-85926-7.

22. Hawthorne, M. F. *et al.* The Preparation and Characterization of the (3)-1,2- and (3) -1,7-Dicarbadodecahydroundecaborate (–1) Ions. *Journal of the American Chemical Society* **90**, 862–868 (1968).

23. Zalkin, A., Hopkins, T. E. & Templeton, D. H. Crystal Structure of Cs(B9C2H11)2Co. *Inorganic Chemistry* **6**, 1911–1915 (1967).

24. Grimes, R. N. Metallacarboranes in the new millennium. *Coordination Chemistry Reviews* **200**–**202**, 773–811 (2000).

25. Warren, L. F. & Hawthorne, M. F. The Chemistry of the Bis[π-3)-1,2-dicarbollyl] Metalates of Nickel and Palladium. *Journal of the American Chemical Society* **92**, 1157–1173 (1970).

26. Clair, D. S., Zalkin, A. & Templeton, D. H. The Crystal Structure of 3,3′-commo-Bis[undecahydro-1,2-dicarba-3-nickela-closo-dodecaborane], a Nickel(IV) Complex of the Dicarbollide Ion1. *Journal of the American Chemical Society* **92**, 1173–1179 (1970).

27. Hawthorne, M. F. *et al.* π-Dicarbollyl Derivatives of the Transition Metals. Metallocene Analogs. *Journal of the American Chemical Society* **90**, 879–896 (1968).

28. Hawthorne, M. F., Young, D. C. & Wegner, P. A. Carbametallic Boron Hydride Derivatives. I. Apparent Analogs of Ferrocene and Ferricinium Ion. *Journal of the American Chemical Society* **87**, 1818–1819 (1965).

29. Bühl, M., Hnyk, D. & Macháček, J. Computational Study of Structures and Properties of Metallaboranes: Cobalt Bis(dicarbollide). *Chemistry - A European Journal* **11**, 4109–4120 (2005).

30. Juárez-Pérez, E. J., Núñez, R., Viñas, C., Sillanpää, R. & Teixidor, F. The Role of C–H···H–B Interactions in Establishing Rotamer Configurations in Metallabis(dicarbollide) Systems. *European Journal of Inorganic Chemistry* **2010**, 2385–2392 (2010).

31. Qi, B. *et al.* From boron clusters to gold clusters: new label-free colorimetric sensors. *Chemical Communications* **53**, 11790–11793 (2017).

32. Tarrés, M. *et al.* Aqueous Self-Assembly and Cation Selectivity of Cobaltabisdicarbollide Dianionic Dumbbells. *Chemistry – A European Journal* **20**, 6786–6794 (2014).

33. Sivaev, I. B., Semioshkin, A. A., Brellochs, B., Sjöberg, S. & Bregadze, V. I. Synthesis of oxonium derivatives of the dodecahydro-closo-dodecaborate anion [B12H12]2-. Tetramethylene oxonium derivative of [B12H12]2- as a convenient precursor for the synthesis of functional compounds for boron neutron capture therapy. *Polyhedron* **19**, 627–632 (2000).

34. Zaulet, A. *et al.* Deciphering the role of the cation in anionic cobaltabisdicarbollide clusters. *Journal of Organometallic Chemistry* **865**, 214–225 (2018).

35. Medoš, Ž. *et al.* Counterion-Induced Aggregation of Metallacarboranes. *Journal of Physical Chemistry C* **126**, 5735–5742 (2022).

36. Plešek, J. *et al.* Potential uses of metallocarborane sandwich anions for analysis, characterization and isolation of various cations and organic bases. *Collection of Czechoslovak Chemical Communications* **49**, 2776–2789 (1984).

37. Knoth, W. H. *et al.* Chemistry of Boranes. IX. Halogenation of B10H10−2 and B12H12−2. *Inorganic Chemistry* **3**, 159–167 (1964).

38. Thomsen, H., Haeckel, O., Krause, U. & Preetz, W. Darstellung und spektroskopische Charakterisierung der Monofluorohydro-closo-Borate [B6H5F]2− und [B12H11F]2−. *Zeitschrift für anorganische und allgemeine Chemie* **622**, 2061–2064 (1996).

39. Ivanov, S. V., Lupinetti, A. J., Solntsev, K. A. & Strauss, S. H. Fluorination of deltahedral closo-borane and -carborane anions with N-fluoro reagents. *Journal of Fluorine Chemistry* **89**, 65–72 (1998).

40. Knoth, W. H., Sauer, J. C., England, D. C., Hertler, W. R. & Mtjetterties, E. L. Chemistry of Boranes. XIX.1 Derivative Chemistry of B10H10-2 and B12H12-. *Journal of the American Chemical Society* **86**, 3973–3983 (1964).

41. Tolpin, E. I., Wellum, G. R. & Berley, S. A. Synthesis and Chemistry of Mercaptoundecahydro-Closo-Dodecaborate(2-). *Inorganic Chemistry* **17**, 2867–2873 (1978).

42. Brattsev, V. A. & Morris, J. H. *Advances in neutron capture therapy*. vol. 2 (Elsevier, 1997).

43. Peymann, T. *et al.* Aromatic Polyhedral Hydroxyborates: Bridging Boron Oxides and Boron Hydrides. *Angew. Chem. Int. Ed* **38**, (1999).

44. Sivaev, I. B., Sjöberg, S., Bregadze, V. I. & Gabel, D. Synthesis of alkoxy derivatives of dodecahydro-closo-dodecaborate anion [B12H12]2−. *Tetrahedron Letters* **40**, 3451–3454 (1999).

45. Peymann, T., Lork, E. & Gabel, D. Hydroxoundecahydro-closo-dodecaborate(2-) as a Nucleophile. Preparation and Structural Characterization of O-Alkyl and O-Acyl Derivatives of Hydroxoundecahydro-closo-dodecaborate(2-). (1996).

46. Haeckel, O. & Preetz, W. Reaktionen von [B12H12-n(OH)n]2-, n = 1, 2 mit Säuredichloriden und Kristallstruktur von Cs2[1,2-B12H10(ox)] · CH3OH. *Zeitschrift für anorganische und allgemeine Chemie* **624**, 1089–1094 (1998).

47. Semioshkin, A. A., Sivaev, I. B. & Bregadze, V. I. Cyclic oxonium derivatives of polyhedral boron hydrides and their synthetic applications. *Journal of the Chemical Society. Dalton Transactions* **11**, 977–992 (2008).

48. Sivaev, I. B. *et al.* Practical synthesis of 1,4-dioxane derivative of the closo-dodecaborate anion and its ring opening with acetylenic alkoxides. *Journal of Organometallic Chemistry* **693**, 519–525 (2008).

49. Nickon, A. & Silversmith, E. F. *Organic Chemistry: The Name Game: Modern Coined Terms and Their Origins*. (Pergamon Press, 2013).

50. Körbe, S., Schreiber, P. J. & Michl, J. Chemistry of the Carba-closo-dodecaborate(-) anion, CB11H12-. *Chemical Reviews* **106**, 5208–5249 (2006).

51. Quan, Y., Tang, C. & Xie, Z. Nucleophilic substitution: A facile strategy for selective B-H functionalization of carboranes. *Dalton Transactions* **48**, 7494–7498 (2019).

52. Hawthorne, M. F. The Role of Chemistry in the Development of Boron Neutron Capture Therapy of Cancer. *Angewandte Chemie International Edition in English* **32**, 950–984 (1993).

53. Imperio, D. *et al.* A Short and Convenient Synthesis of closo-Dodecaborate Sugar Conjugates. *European Journal of Organic Chemistry* **2019**, 7228–7232 (2019).

54. Kabalka, G. W. & Yao, M.-L. The Synthesis and Use of Boronated Amino Acids for Boron Neutron Capture Therapy. *Anti-Cancer Agents in Medicinal Chemistry* **6**, 111–125 (2006).

55. Byun, Y. *et al.* 3-Carboranyl Thymidine Analogues (3CTAs) and Other Boronated Nucleosides for Boron Neutron Capture Therapy. *Anti-Cancer Agents in Medicinal Chemistry* **6**, 127–144 (2006).

56. Feakes, D. A., Spinler, J. K. & Harris, F. R. Synthesis of boron-containing cholesterol derivatives for incorporation into unilamellar liposomes and evaluation as potential agents for BNCT. *Tetrahedron* **55**, 11177–11186 (1999).

57. Bregadze, V. I., Sivaev, I. B., Gabel, D. & Wöhrle, D. Polyhedral boron derivatives of porphyrins and phthalocyanines. *Journal of Porphyrins and Phthalocyanines* **5**, 767–781 (2001).

58. Hawthorne, M. F. & Maderna, A. Applications of Radiolabeled Boron Clusters to the Diagnosis and Treatment of Cancer. *Chemical Reviews* **99**, 3421–3434 (1999).

59. Yamamoto, Y. Boron-gadolinium binary system as a magnetic resonance imaging boron carrier. *Pure and Applied Chemistry* **75**, 1343–1348 (2003).

60. Rutten, A. & Prokop, M. Contrast Agents in X-Ray Computed Tomography and Its Applications in Oncology. *Anti-Cancer Agents in Medicinal Chemistry* **7**, 307–316 (2007).

61. Martin Jimenez, J. L. *et al.* New iodized boron compounds useful as X ray contrasting agents, and pharmaceutical compositions containing them. (1996).

62. Barba-Bon, A. *et al.* Boron clusters as broadband membrane carriers. *Nature* **603**, 637–642 (2022).

63. Chen, Y. *et al.* Metallacarborane Cluster Anions of the Cobalt Bisdicarbollide-Type as Chaotropic Carriers for Transmembrane and Intracellular Delivery of Cationic Peptides. *Journal of the American Chemical Society* **145**, 13089–13098 (2023).

64. Fink, K. & Uchman, M. Boron cluster compounds as new chemical leads for antimicrobial therapy. *Coordination Chemistry Reviews* vol. 431 213684 (2021).

65. Kožíšek, M. *et al.* Inorganic Polyhedral Metallacarborane Inhibitors of HIV Protease: A New Approach to Overcoming Antiviral Resistance. *Journal of Medicinal Chemistry* **51**, 4839–4843 (2008).

66. Cígler, P. *et al.* From nonpeptide toward noncarbon protease inhibitors: Metallacarboranes as specific and potent inhibitors of HIV protease. *Proceedings of the National Academy of Sciences* **102**, 15394–15399 (2005).

67. Kaszynski, P. & G. Douglass, A. Organic derivatives of closo-boranes: a new class of liquid crystal materials. *Journal of Organometallic Chemistry* **581**, 28–38 (1999).

68. Allis, D. G. & Spencer, J. T. Polyhedral-Based Nonlinear Optical Materials. 2. 1 Theoretical Investigation of Some New High Nonlinear Optical Response Compounds Involving Polyhedral Bridges with Charged Aromatic Donors and Acceptors. *Inorganic Chemistry* **40**, 3373–3380 (2001).

69. Li, J. *et al.* Polynorbornene-Based Polyelectrolytes with Covalently Attached Metallacarboranes: Synthesis, Characterization, and Lithium-Ion Mobility. *Macromolecules* **54**, 6867–6877 (2021).

70. Plesek, J. Potential applications of the boron cluster compounds. *Chemical Reviews* **92**, 269–278 (1992).

71. Hurlburt, P. K. *et al.* New synthetic routes to B-halogenated derivatives of cobalt dicarbollide. *Inorganic Chemistry* **34**, 5215–5219 (1995).

72. Bernard, R. *et al.* Synthesis of [B12H12]2− based extractants and their application for the treatment of nuclear wastes. *Journal of Organometallic Chemistry* **657**, 83–90 (2002).

73. Belmont, J. A. *et al.* Metallacarboranes in catalysis. 8. I: Catalytic hydrogenolysis of alkenyl acetates. II: Catalytic alkene isomerization and hydrogenation revisited. *Journal of the American Chemical Society* **111**, 7475–7486 (1989).

74. Tutusaus, O. *et al.* Half-sandwich ruthenium complexes for the controlled radical polymerisation of vinyl monomers. *Inorganic Chemistry Communications* **5**, 941–945 (2002).

75. Yoshida, M., Crowther, D. J. & Jordan, R. F. Synthesis, Structure, and Reactivity of a Novel Hafnium Carboranyl Hydride Complex. *Organometallics* **16**, 1349–1351 (1997).

76. Wang, J., Steenhaut, T., Li, H.-W. & Filinchuk, Y. High Yield Autoclave Synthesis of pure M 2 B 12 H 12 (M = Na, K). *Inorganic Chemistry* **62**, 2153–2160 (2023).

77. Bennour, I., Cioran, A. M., Teixidor, F. & Viñas, C. 3,2,1 and stop! An innovative, straightforward and clean route for the flash synthesis of metallacarboranes. *Green Chemistry* **21**, 1925–1928 (2019).

78. Lee, Y. S. *Self-Assembly and Nanotechnology: A Force Balance Approach*. (John Wiley & Sons, 2007).

79. Ďorďovič, V. *et al.* Stealth Amphiphiles: Self-Assembly of Polyhedral Boron Clusters. *Langmuir* **32**, 6713–6722 (2016).

80. Assaf, K. I. & Nau, W. M. The Chaotropic Effect as an Assembly Motif in Chemistry. *Angewandte Chemie International Edition* **57**, 13968–13981 (2018).

81. Fernandez-Alvarez, R., Ďorďovič, V., Uchman, M. & Matějíček, P. Amphiphiles without Head-and-Tail Design: Nanostructures Based on the Self-Assembly of Anionic Boron Cluster Compounds. *Langmuir* **34**, 3541–3554 (2018).

82. Matějíček, P. *et al.* On the Structure of Polymeric Composite of Metallacarborane with Poly(ethylene oxide). *Macromolecules* **44**, 3847–3855 (2011).

83. Matějíček, P. *et al.* Stimuli-Responsive Nanoparticles Based on Interaction of Metallacarborane with Poly(ethylene oxide). *Macromolecules* **42**, 4829–4837 (2009).

84. Ďorďovič, V. *et al.* Hybrid Nanospheres Formed by Intermixed Double-Hydrophilic Block Copolymer Poly(ethylene oxide)- block -poly(2-ethyloxazoline) with High Content of Metallacarboranes. *Macromolecules* **46**, 6881–6890 (2013).

85. Wang, W. *et al.* The chaotropic effect as an orthogonal assembly motif for multi-responsive dodecaborate-cucurbituril supramolecular networks. *Chemical Communications* **54**, 2098–2101 (2018).

86. Fernandez-Alvarez, R. *et al.* Interactions of star-like polyelectrolyte micelles with hydrophobic counterions. *Journal of Colloid and Interface Science* **546**, 371–380 (2019).

87. Li, J. *et al.* Designed Boron-Rich Polymeric Nanoparticles Based on Nano-ion Pairing for Boron Delivery. *Chemistry – A European Journal* **26**, 14283–14289 (2020).

88. Li, J. *et al.* Engineered nanogels shape templated by closo-dodecaborate nano-ion and dictated by chemical crosslinking for efficient boron delivery. *Journal of Molecular Liquids* **336**, 116367 (2021).

89. Günther, H. *NMR Spectroscopy: Basic Principles, Concepts and Applications in Chemistry*. (Wiley-VCH Verlag GmbH, 2013).

90. Dračínský, M. *NMR spektroskopie pro chemiky*. (Knihovna chemie Přírodovědecké fakulty UK, 2021).

91. Morris, G. A. Diffusion-Ordered Spectroscopy. in *Encyclopedia of Magnetic Resonance* (John Wiley & Sons, Ltd, 2009). doi:10.1002/9780470034590.emrstm0119.pub2.

92. Gross, J. H. *Mass Spectrometry: A textbook*. (Springer International Publishing, 2017). doi:10.1007/978-3-319-54398-7.

93. de Hoffmann, E. & Stroobant, V. *Mass Spectrometry: Principles and Applications*. (John Wiley & Sons, Ltd, 2007).

94. Schärtl, W. *Light Scattering from Polymer Solutions and Nanoparticle Dispersions*. (Springer Berlin Heidelberg, 2007). doi:10.1007/978-3-540-71951-9.

95. Munk, P. & Aminabhavi, T. M. *Introduction to Macromolecular Science*. (John Wiley & Sons, Inc, 2002).

96. Armarego, W. L. F. *Purification of laboratory chemicals*. (Butterworth-Heinemann, 2003).

97. Jerschow, A. & Müller, N. Suppression of Convection Artifacts in Stimulated-Echo Diffusion Experiments. Double-Stimulated-Echo Experiments. *Journal of Magnetic Resonance* **125**, 372–375 (1997).

98. Hleli, B. *et al.* Closo-dodecaborate-based dianionic surfactants with distorted classical morphology: Synthesis and atypical micellization in water. *Journal of Colloid and Interface Science* **648**, 809–819 (2023).

99. Grüner, B. & Plzák, Z. High-performance liquid chromatographic separations of boron-cluster compounds. *Journal of Chromatography A* **789**, 497–517 (1997).